ISTANBUL TECHNICAL UNIVERSITY ★ GRADUATE SCHOOL

# EXTERNAL STORE SEPARATION FROM FIGHTER AIRCRAFT

**M.Sc. THESIS**

**Ahmet Kutsay DERE**

**Department of Aeronautical and Astronautical Engineering**

**Aeronautical and Astronautical Engineering Programme**

**JUNE 2025**

**ISTANBUL TECHNICAL UNIVERSITY ★ GRADUATE SCHOOL**

# EXTERNAL STORE SEPARATION FROM FIGHTER AIRCRAFT

**M.Sc. THESIS**

**Ahmet Kutsay DERE**
**(511201106)**

**Department of Aeronautical and Astronautical Engineering**

**Aeronautical and Astronautical Engineering Programme**

**Thesis Advisor: Assis. Prof. Dr. Hayri ACAR**

**JUNE 2025**

**ISTANBUL TEKNİK ÜNİVERSİTESİ ★ LİSANSÜSTÜ EĞİTİM ENSTİTÜSÜ**

# SAVAŞ UÇAĞINDAN HARİCİ MÜHİMMATIN AYRILMASI

**YÜKSEK LİSANS TEZİ**

**Ahmet Kutsay DERE**
**(511201106)**

**Uçak ve Uzay Mühendisliği Anabilim Dalı**

**Uçak ve Uzay Mühendisliği Programı**

**Tez Danışmanı: Doç. Dr. Hayri ACAR**

**HAZİRAN 2025**

Ahmet Kutsay DERE, a M.Sc. student of ITU Graduate School student ID 511201106, successfully defended the thesis/dissertation entitled "EXTERNAL STORE SEPARATION FROM FIGHTER AIRCRAFT", which he prepared after fulfilling the requirements specified in the associated legislations, before the jury whose signatures are below.

| | | |
|---|---|---|
| **Thesis Advisor:** | **Assis. Prof. Dr. Hayri ACAR**<br>İstanbul Technical University | .............................. |
| **Jury Members:** | **Assis. Prof. Dr. Ramazan YENİÇERİ**<br>İstanbul Technical University | .............................. |
| | **Assis. Prof. Dr. Serhat YILMAZ**<br>National Defence University | .............................. |

**Date of Submission : 30 May 2025**
**Date of Defence : 24 June 2025**

***To my beloved family,***

## FOREWORD

I would like to express my deepest gratitude to my teacher Assoc. Prof. Dr. Hayri ACAR for the trust and endless support he gave me.
I would like to thank my colleagues in Turkish Aerospace Industries, Kaan ÜÇKÖK, Malik ÇELİK, Ertuğrul FALCI and Fazıl Selçuk GÖMEÇ because of their support to my study. They supported me in obtaining the aerodynamic database for store separation and also guided me through the difficulties I had in store separation analysis.
I am grateful, especially my chief engineer Arda ÇALIŞKAN for his guidance and advices he gave me.
Additionally,
I am so grateful to my lovely wife Nur Efşan and my sweetheart Hafsa Hüma for their patience, endless support and love. I feel so lucky to have her and I couldn't have done any of this without her.
Finally,
I would like to thank my parents for all their sacrifices and efforts throughout my education. I feel very lucky to have them.

May 2025

Ahmet Kutsay DERE
Aeronautical Engineer

**TABLE OF CONTENTS**

**Page**

## ABBREVIATIONS

| | |
|---|---|
| **AABB** | **:** Axis-Aligned Bounding Box Method |
| **AoA** | **:** Angle of Attack |
| **AFSEO** | **:** USAF SEEK EAGLE Office |
| **CAD** | **:** Computer Aided Design |
| **CFD** | **:** Computational Fluid Dynamics |
| **CG** | **:** Center of Gravity |
| **CTS** | **:** Captive Trajectory System |
| **D (1D, 2D)** | **:** Dimension |
| **deg** | **:** Degree |
| **DOF** | **:** Degree of Freedom |
| **ft** | **:** Feet |
| **GBU** | **:** Guided Bomb Unit |
| **lbf** | **:** Pound-Force |
| **m** | **:** Meter |
| **MATLAB** | **:** Matrix Laboratory |
| **MIL-HDBK** | **:** Military Handbook |
| **NATO** | **:** North Atlantic Treaty Organization |
| **SAT** | **:** Separated Axis Theorem |
| **TUSAŞ** | **:** Turkish Aerospace Industries |
| **U.S.** | **:** United States of America |

**SYMBOLS**

| | |
|---|---|
| $g$ | : Gravitational Acceleration |
| $m$ | : Mass (kg or slug) |
| $x$ | : North Position |
| $y$ | : East Position |
| $z$ | : Down Position |
| p | : Roll Rate |
| $q$ | : Pitch Rate |
| $r$ | : Yaw Rate |
| u | : X Body Velocity |
| $v$ | : Y Body Velocity |
| ω | : Z Body Velocity |
| $\phi$ | : Euler Roll Angle |
| $\theta$ | : Euler Pitch Angle |
| $\psi$ | : Euler Yaw Angle |
| $F_x$ | : Body Axis X Force |
| $F_y$ | : Body Axis Y Force |
| $F_z$ | : Body Axis Z Force |
| $M_x$ | : Roll Moment |
| $M_y$ | : Pitch Moment |
| $M_z$ | : Yaw Moment |
| $I_{xx}$ | : Moment of Inertia about X Body Axis |
| $I_{yy}$ | : Moment of Inertia about Y Body Axis |
| $I_{zz}$ | : Moment of Inertia about Z Body Axis |
| $I_{xy}$ | : Product of Inertia in X Body - Y Body Axis |
| $I_{xz}$ | : Product of Inertia in X Body - Z Body Axis |
| $I_{yz}$ | : Product of Inertia in Y Body - Z Body Axis |
| $Cl_p$ | : Roll Damping Coefficient |
| $Cm_q$ | : Pitch Damping Coefficient |
| $Cn_r$ | : Yaw Damping Coefficient |

| | |
|---|---|
| $\boldsymbol{X_{CG}}$ | : Center of Gravity Position in Store Body X Axis |
| $\boldsymbol{X_{FE}}$ | : Forward Ejector Position in Store Body X Axis |
| $\boldsymbol{X_{AE}}$ | : Aftward Ejector Position in Store Body X Axis |
| $\boldsymbol{b}$ | : Reference Wing Span |
| $\boldsymbol{s}$ | : Reference Wing Area |
| $\boldsymbol{\bar{c}}$ | : Mean Aerodynamic Chord |
| $\boldsymbol{x_{cg}}$ | : X CG location |
| $\boldsymbol{x_{cg_r}}$ | : Reference X CG location |
| $\boldsymbol{M}$ | : Mach |
| $\boldsymbol{h}$ | : Altitude (kft) |
| $\boldsymbol{\gamma}$ | : Flight Path Angle (deg) |
| $\boldsymbol{\alpha}$ | : Angle of Attack (deg) |
| $\boldsymbol{\beta}$ | : Angle of Sideslip (deg) |
| $\boldsymbol{N_z}$ | : Normal load factor (g) |
| $\boldsymbol{T}$ | : Time (s) |
| $\boldsymbol{CAT}$ | : Store Aerodynamic Axial Force Coefficient |
| $\boldsymbol{CN}$ | : Store Aerodynamic Normal Force Coefficient |
| $\boldsymbol{CY}$ | : Store Aerodynamic Side Force Coefficient |
| $\boldsymbol{CLL}$ | : Store Aerodynamic Rolling Moment Coefficient |
| $\boldsymbol{CLM}$ | : Store Aerodynamic Pitching Moment Coefficient |
| $\boldsymbol{CLN}$ | : Store Aerodynamic Yawing Moment Coefficient |
| $\boldsymbol{FE1}$ | : Forward Ejector Force (lbf) |
| $\boldsymbol{FE2}$ | : Aft Ejector Force (lbf) |

**LIST OF TABLES**

**Page**

## LIST OF FIGURES

**Page**

**EXTERNAL STORE SEPARATION FROM FIGHTER AIRCRAFT**

## SUMMARY


Modern fighter aircraft carry various external stores, such as munitions, fuel tanks, and pods, under the fuselage or wings to complete missions successfully. The safe and stable release of these stores is very important for both mission success and flight safety. This process is called store separation. It is affected by the aerodynamics of the aircraft, the shape of the store, the flight conditions, and the physical properties of the release mechanisms.

During separation, the store is affected by aerodynamic forces and moments. These forces determine the path and orientation of the store, and also the risk of collision with the aircraft. Therefore, the separation process must be carefully analyzed. It is not only about the mechanical release system, but also how the store behaves at subsonic, transonic, or supersonic speeds. The store must separate safely and also fly stably toward the target.

In practice, various methods can be preferred for store separation analysis:

- Wind Tunnel Test
- Flight Test
- Store Separation Simulations

Flight tests give the most accurate results, but they are very expensive, takes time, and can only test limited scenarios. In a wind tunnel test, the aircraft and store are tested together to measure aerodynamic loads during separation. Trajectory of the store calculated for each flight case by doing 6 DOF simulation. Wind tunnel tests are also costly and slow.

Computational Fluid Dynamics (CFD) based 6-Degree-of-Freedom (6-DoF) simulations are widely used to understand the aerodynamic behavior of the store during release. Methods like Grid Method and Overset Grid help calculate the aerodynamic forces and moments at different positions of the store, so the separation can be analyzed.

Munitions are usually divided into two groups: bombs and missiles. They use different release systems. Bombs fall due to gravity and ejector forces. Missiles also have rocket motors that give forward speed.

Stores can be carried on internal stations inside the fuselage or on external stations under the wings. In this study, the store is a free-falling bomb, released from an external wing station. Separation from internal stations is harder than from external

stations. The airflow inside the cavity is unsteady and affects the separation more. However, cavity flow is out of scope for this study.

In this thesis, aerodynamic interactions between the store and the aircraft during separation are studied. The factors that affect safe separation are discussed using numerical modeling and trimming techniques. Simulation results show how store separation changes in different flight conditions. The goal is to support store design and integration and to help decide the best release moment.

.

**SAVAŞ UÇAĞINDAN HARİCİ MÜHİMMATIN GÜVENLİ AYRILMASI**

## ÖZET

Modern savaş uçakları, görevlerini etkili bir şekilde yerine getirebilmek için, çeşitli harici yükleri, mühimmat, yakıt tankı, pod gibi, gövde ya da kanat altına entegre edilmiş şekilde taşımaktadır. Bu harici yükler, uçuş sırasında hem uçağın performansını hem de görev başarısını doğrudan etkileyebilecek niteliktedir. Bu nedenle, yüklerin güvenli bir şekilde uçağa entegre edilmesi, uçuş güvenliği ile doğrudan ilişkili olup, uçaktan ayrılmaları süreci de oldukça kritik bir aşama teşkil etmektedir. Mühimmat ayrılması (store separation) olarak adlandırılan bu süreç, mühimmatın uçaktan ayrıldığı andan itibaren uçuş güvenliği açısından kritik öneme sahiptir. Mühimmatın uçaktan doğru bir şekilde ayrılabilmesi hem mühimmatın hedefe ulaşabilmesi hem de taşıyıcı uçağın güvenli bir şekilde görevini sürdürebilmesi için gereklidir.

Mühimmat ayrılma süreci, birçok faktörden etkilenmektedir. Uçağın aerodinamik yapısı, mühimmatın geometrisi, uçuş zarfı koşulları ve mühimmatın ayrılmasını sağlayan mekanizmaların fiziksel özellikleri, bu süreci doğrudan etkileyen unsurlardır. Ayrılma sırasında, mühimmatın uçaktan ayrıldığı an ve sonrasında maruz kaldığı aerodinamik kuvvetler, momentler ve etkileşimler, mühimmatın izlediği yörüngeyi, yönelimini ve taşıyıcı uçağa olan mesafesini belirleyen temel faktörlerdir. Bu kuvvetlerin, mühimmatın uçaktan ayrıldıktan sonraki davranışını etkilemesi, uçuş güvenliği ve görev başarısı açısından son derece önemlidir. Mühimmat ayrılma süreci, sadece mekanik salım sistemlerinin doğru çalışması ile değil, aynı zamanda mühimmatın ayrılma sonrasında altsonik, transonik ya da süpersonik hızlarda nasıl davrandığının titizlikle analiz edilmesiyle güvence altına alınmalıdır. Mühimmatın, uçaktan güvenli bir şekilde ayrılmasının yanı sıra, ayrıldıktan sonra hedefe doğru istikrarlı ve kararlı bir şekilde yönelmesi de büyük önem taşır. Bu durum, özellikle savaş uçakları ve mühimmatın yüksek hızlarla seyir halinde olduğu senaryolarda, ayrılma anından sonra mühimmatın hedefe ulaşmasını engelleyecek kararsızlıkların önlenmesini gerektirir.

Pratik uygulamalarda mühimmat ayrılma analizinde kullanılan çeşitli yöntemler ve teknikler, bu sürecin güvenli ve doğru bir şekilde gerçekleştirilmesini sağlamaya yönelik olarak geliştirilmiştir. Bu analizlerde, farklı test ve simülasyon yöntemleri tercih edilebilir. Bu yöntemlerden bazıları şunlardır:

- **Rüzgar Tüneli Testleri:** Bu testler, uçak ve mühimmat arasındaki aerodinamik etkileşimleri daha ayrıntılı şekilde incelemeye olanak tanır. Rüzgar tünelinde yapılan testler, mühimmatın ayrılma sırasında maruz kaldığı aerodinamik yüklerin ölçülmesini sağlar. Bu yüklerin etkisi altında mühimmatın izlediği yörüngeyi, hızlanma değerlerini ve uçuş yönelimini detaylı bir şekilde analiz etmek mümkündür. Ancak rüzgar tüneli testleri oldukça pahalıdır, zaman alıcıdır ve sadece sınırlı sayıda senaryoda geçerlidir.
- **Uçuş Testleri:** Uçuş testleri, mühimmat ayrılma sürecini gerçek dünya koşullarında test etmenin en doğru yöntemlerinden biridir. Bu testlerde, mühimmatın uçaktan ayrıldıktan sonraki davranışı gözlemlenir ve kaydedilir. Uçuş testleri, laboratuvar ortamında yapılan simülasyonlardan daha gerçekçi sonuçlar verebilir, ancak maliyetli, zaman alıcı ve sınırlı sayıda test yapmaya olanak tanır. En önemlisi uçuş güvenliği açısından riskler barındırır.
- **Mühimmat Ayrılma Simülasyonları:** Bu tür simülasyonlar, hesaplamalı akışkanlar dinamiği (CFD) gibi sayısal yöntemler kullanılarak yapılır. Simülasyonlar, mühimmatın aerodinamik davranışını daha ayrıntılı bir şekilde analiz etmeyi sağlar. Mühimmatın uçaktan ayrıldıktan sonra izlediği yol, hız ve yönelim gibi parametreler bu simülasyonlarla daha güvenli bir şekilde tahmin edilebilir.

Hesaplamalı Akışkanlar Dinamiği (CFD) tabanlı 6 Serbestlik Derecesi (6-DoF) simülasyonları, mühimmatın serbest bırakılma anındaki aerodinamik davranışını incelemek için yaygın olarak kullanılan bir tekniktir. Bu simülasyonlar sayesinde, mühimmatın ayrılma anında maruz kaldığı kuvvetler ve momentler, sayısal ağ tabanlı çözümler kullanılarak hesaplanır. Bu tür çözümler, mühimmatın uçaktan ayrılma sonrasındaki davranışını daha ayrıntılı bir şekilde analiz etmeye yardımcı olur. Örneğin, mühimmatın havada sabit bir yörüngede ilerlemesi veya taşınan hızlarla etkileşimde bulunarak yön değiştirmesi gibi durumlar simülasyonlarda test edilebilir.

Mühimmatlar, genellikle bombalar ve füzeler olmak üzere iki ana kategoride sınıflandırılabilir. Bu mühimmat türleri, bırakılma mekanizmaları açısından farklılık gösterirler. Bombalar, çoğunlukla kendi ağırlıkları ve fırlatma kuvvetleri etkisinde serbest düşüş hareketi yaparak hedeflerine doğru ilerlerken, füzeler ise motorlar sayesinde ileri yönde hızlanarak hedeflerine ulaşırlar. Bu iki farklı mühimmat tipi, mühimmat ayrılma sürecinde farklı aerodinamik etkileşimlere yol açar ve her birinin kendine özgü ayrılma mekanizmaları vardır. Ayrıca mühimmatlar, uçağın gövdesi içerisindeki iç istasyonlarda veya kanat altındaki dış istasyonlarda taşınabilir. İç istasyonlardan ayrılma, dış istasyonlara göre daha zorlu bir süreçtir, çünkü iç istasyonlardan ayrılma sırasında akış kararsızlıkları daha belirgin hale gelir ve aerodinamik etkiler bu noktada çok daha karmaşık bir yapıya bürünür. Ancak bu çalışmada, özellikle iç istasyonlardan ayrılma detaylarına odaklanılmamış, dış istasyonlardan ayrılma süreci üzerinde durulmuştur.

Bu tez çalışmasında, savaş uçaklarından ayrılan mühimmatların uçakla olan aerodinamik etkileşimleri detaylı bir şekilde incelenmiştir. Bu etkileşimlerin güvenli mühimmat ayrılması üzerindeki etkileri, sayısal modelleme ve trimleme yaklaşımlarıyla değerlendirilmiştir. Simülasyon sonuçları, mühimmat ayrılmasının farklı uçuş koşullarında nasıl değiştiğini ve hangi uçuş senaryolarında güvenli mühimmat ayrılması sağlanabileceğini ortaya koymuştur. Bu veriler, mühimmat tasarımı ve entegrasyonu süreçlerine katkı sağlamayı amaçlamakta olup, mühimmatların tasarımında güvenli ayrılma koşullarının göz önünde bulundurulmasını teşvik etmektedir. Ayrıca, mühimmatın güvenli bir şekilde ayrılabilmesi için hangi anda bırakılması gerektiği konusunda da önemli kararlar verilmesi sağlanmıştır. Bu kararlar, mühimmatın hedefe ulaşma olasılığını en üst düzeye çıkarmayı ve taşıyıcı uçağın güvenliğini tehlikeye atmadan mühimmatın doğru şekilde işlev görmesini sağlamayı hedeflemektedir.

# 1. INTRODUCTION

## 1.1 Motivation Behind the Study

In recent years, the development of fighter jets and munitions in our country has increased the importance of safe store separation studies. Developing a new aircraft consists of many challenging topics including carrying and employing of stores. Aircraft must be designed to enable safe separation of new designed or currently used stores. Using 6-DOF model simulations is very useful to test store separation scenarios and choose the suitable ones. This method avoids the disadvantages of flight tests and wind tunnel tests. After getting aerodynamic forces and moments from CFD software, many release simulations can be done under different flight conditions using 6-DOF models. Running many simulations does not cause extra time or cost.

In this study, only a bomb-type store (free-falling and without propulsion) is analyzed for safe separation. However, the same method can also be used for missile-type stores, which have their own propulsion. Also, this study focuses on a store carried on an external station. But with the addition of internal flow effects, the same method can be used to study releases from internal stations as well.

## 1.2 Outline of the Thesis

In this study, store release analyses will be conducted under various flight scenarios. The separation of the store from the aircraft will be monitored up to a certain vertical distance, during which the risk of collision with the aircraft will be evaluated.

In Chapter 1.3, a literature review will be presented, outlining the previous studies on store separation conducted up to this work. Then, the methods for obtaining the aerodynamic data necessary for store separation will be explained. In this section, the Grid Method, Flow Field Method, and Captive Trajectory Simulation (CTS) Method will be discussed.

The following chapter will cover the selection of the ejector system and explain the store's carriage and release envelopes.

In Chapter 2, the 6-DOF simulation model developed for the store will be described. The frames used in this model and the equations of motion will be presented. Then, the implementation of the 6-DOF model will be explained.

Chapter 3 will introduce the Eglin store geometry used for validation purposes. After explaining how the aerodynamic data for the Eglin test case was obtained, the flight data resulting from this test will be shared. In the final part of this section, simulation outputs from the 6-DOF model using the initial conditions of the Eglin scenario will be compared with actual Eglin data, and model validation will be performed.

Chapter 4 will provide details about the aircraft used to generate the aerodynamic grid data for safe separation analysis.

In Chapter 5, an F-16 6-DOF model will be introduced to both generate the initial conditions for the store separation and to create an aircraft model that moves relative to the store. Trim process of F-16 aircraft under various flight conditions will also be described.

Chapter 6 will focus on the store separation topic. Simulations will be carried out using the trimmed conditions of the F-16 aircraft and the aerodynamic data of the fifth-generation aircraft and the Eglin pylon-store configuration. In these simulations, the aircraft and the store will move independently with respect to the ground, and their positions, velocities, and attitude changes will be analyzed to determine whether the separation is safe. In Chapter 6.1, a basic collision detection method will be introduced. Rectangular boxes will be assigned to both the aircraft and the store, and intersections between these volumes will be checked at each simulation step. Based on this analysis, safe and unsafe release conditions will be identified.

Chapter 7 includes separation analysis results, comments about the results and future works. Separation graphics are shown in Chapter 7.1-7.2 and 7.3

## 1.3 Literature Review

Store separation is a critical engineering problem in terms of mission effectiveness and flight safety for combat aircraft. This problem involves an interdisciplinary combination of aerodynamics, structural mechanics, control systems, and mechanical design. The trajectory followed by the store after it separates from the aircraft must be both safe and predictable, in order to ensure that the store can fulfill its mission without causing any harm to the carrier aircraft.

The first comprehensive studies in this field were conducted by the U.S. Air Force in the 1960s and 1970s, focusing on the unstable behaviors observed during store separation. These efforts led to the development of numerical and experimental modeling techniques [1]. In the following years, methods used for store separation analysis evolved from basic 2D aerodynamic calculations to computational fluid dynamics (CFD) and six-degree-of-freedom (6DoF) motion simulations.

The store separation tests carried out at Eglin Air Force Base in the U.S. have become commonly referenced datasets in the literature [2]. These tests document the separation behavior of various stores (e.g., MK-82, GBU-12) released from fighter aircraft under different flight conditions. Such data are widely used to validate CFD solutions. One of the documents where this data is published will also be used in this study for validation purposes: "*CFD Wing Pylon Finned Store Mutual Interference"* [2].

In the CFD-based modeling of store separation, the Grid Method is commonly used. In this approach, separate meshes are generated for each position of the store to estimate the aerodynamic forces and moments. Prashanth and Sucheendran. (2014) showed that the trajectory of the store can be accurately predicted using the grid method [3]. However, the major disadvantage of this method is the high computational cost and time requirement.

To overcome this limitation, the Overset Grid (Chimera mesh) technique was developed. In this method, separated grids are defined for the store and the aircraft, and these grids are overlapped to perform the solution. This avoids the need to regenerate the main grid during the store's motion. The overset grid approach offers advantages in terms of both accuracy and computational efficiency for store separation simulations.

In recent years, artificial intelligence-based modeling approaches have also been applied in store separation analysis. Particularly, machine learning techniques have been used to model CFD results and perform faster simulations [4].

In many of the studies reviewed in the literature, the Eglin store was integrated either beneath various aircraft types or under the Eglin wing geometry. Using a CFD-based Captive Trajectory Simulation (CTS) method, the aerodynamic loads on the store are calculated at each step, and the store is then moved accordingly. The aerodynamic loads at the next position are calculated based on the updated location. In this way, the trajectory resulting from the separation under a specific flight condition is obtained [5].

This study differs from previous works in the literature by performing trim and separation analyses under different flight conditions.

### 1.3.1 Aerodynamic database construction methods

#### 1.3.1.1 Captive trajectory system

The CTS (Captive Trajectory System) method can be performed using wind tunnel tests or CFD analyses. In this method, the aircraft and the store are held in their initial positions, and the analysis begins. At the first moment, aerodynamic loads acting on the store are calculated and recorded. Using these loads, together with ejector forces and the weight of the store, the next position of the store is computed using a 6-DOF model. The sting holding the store is moved to this new position and orientation. At this new location, the aerodynamic loads acting on the store are again computed. Based on these loads, the next position of the store is calculated. This process continues until the store reaches a defined vertical distance from the aircraft. As a result, the trajectory of the store for that specific flight condition is obtained. This method gives more accurate results compared to the Grid and Flow field methods described below; however, it has a longer processing time and only provides data for a single flight condition. It is not possible to reuse the results for other flight conditions. Figure 1.1 shows a CTS mechanism.

An alternative use of the CTS method does not involve a 6-DOF simulation. Instead, the store is moved along a predefined trajectory, and aerodynamic loads acting on the store are measured during this motion.

aerodynamic limits are reached before the blade structural limits. In other words, the curve for McHugh represents pure aerodynamic limitations which means rotor maximum thrust boundary [5].

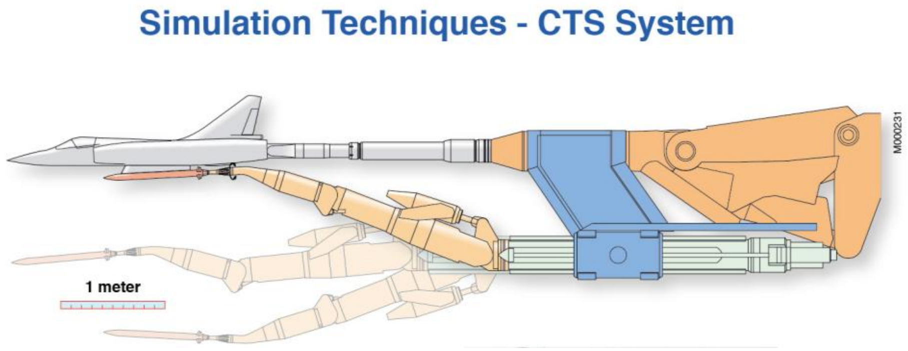


**Figure 1.1 :** Captive trajectory system (CTS) wind tunnel test mechanism

#### 1.3.1.2 Grid method

Accurate determination of the aerodynamic forces and moments acting on a store during its separation from an aircraft is crucial for the success of safe separation analyses. One of the most widely used and effective techniques for this purpose is the Grid Method. This method involves constructing a spatial and angular grid in which the store is positioned at various locations and orientations relative to the aircraft fuselage. At each grid point, the aerodynamic forces and moments acting on the store are computed.

The grid method is applied by considering the 6 degrees of freedom (6-DOF) motion of the store prior to or during separation. In this scope, the store's positions (x, y, z) and orientations (pitch θ, yaw ψ, roll φ) relative to the aircraft reference frame are sampled at a certain resolution. At each sampling point, the aerodynamic forces (F_x, F_y, F_z) and moments (M_x, M_y, M_z) acting on the store are generally calculated using Computational Fluid Dynamics (CFD) methods and recorded in a lookup table. During simulation, the aerodynamic loads at intermediate positions are obtained by interpolation from this database and applied in the equations of motion of the store.

The aerodynamic datasets obtained with this method provide continuous and high-fidelity aerodynamic modelling in separation scenarios. This allows for the prediction of critical safety risks such as collisions with the aircraft, loss of control, or undesired rotational motion.

However, the grid method does not provide results as accurate as the CTS method, because it is not feasible to compute aerodynamic data for every possible position and orientation that the store might occupy. As a result, interpolation must be applied for intermediate positions and orientations, which reduces data fidelity. Nevertheless, with a sufficiently large and dense grid dataset, store separation simulations can still be conducted with acceptable accuracy.

As the grid resolution increases, both the computational cost and the data storage requirements also increase. Moreover, this method does not directly account for unsteady aerodynamic effects.

In this thesis, the separation of a store modelled using the Eglin store geometry from a fifth-generation fighter aircraft was analyzed under various flight conditions. The aerodynamic forces and moments acting on the store during separation were obtained from a database constructed using the grid method and applied in a 6-DOF dynamic model.

#### 1.3.1.3 Flow field method

Modeling and analyzing the dynamic behavior of airflow around the store and the carrier aircraft during store separation plays a critical role in ensuring separation safety. In this context, the Flow-Field Method is a comprehensive approach that involves the direct numerical solution of the fluid field surrounding the store and aircraft.

The Flow-Field Method refers to modelling the airflow around the aircraft and store geometries during separation by solving fundamental fluid dynamics equations, such as the Navier-Stokes equations. In this approach, the aircraft and store geometries are modelled together, and the interactive flow structure is computed with all its physical characteristics (e.g., pressure, velocity, turbulence, vortices). Thus, the aerodynamic forces and moments acting on the store during separation are directly obtained.

The Flow-Field Method is generally preferred in high-fidelity store separation simulations. In this method, the carrier aircraft and the store are modelled simultaneously, and the unsteady and complex flow structures that occur during the separation process are resolved. At each time step of the separation movement, the flow field is updated, and the store’s dynamic motion is simulated using the updated aerodynamic forces.

This method is particularly effective in analyzing complex flow phenomena, such as cavity turbulence and interactions, which are commonly encountered during the separation of stores from internal carriage stations.

Although the Flow-Field Method provides high accuracy and physically represents actual flow conditions, it was not directly used in this thesis. Instead, the more practical Grid Method was chosen to determine the aerodynamic forces between the aircraft and the store. However, for future studies, the Flow-Field Method is expected to provide significant contributions, especially in separation analyses involving internal carriage stations.

### 1.3.2 Ejector selection

In modern fighter aircraft, the safe and stable separation of stores is critically important for both mission success and flight safety. During this process, the aerodynamic forces and moments acting on the store at the moment of release determine the store's trajectory, orientation, and the potential risk of collision with the carrier aircraft. Therefore, the correct selection of the ejector systems used in store separation is of great importance [6].

#### 1.3.2.1 Types of ejectors and their characteristics

The ejector systems used in store separation are generally classified into three main categories:

- Pyrotechnic Ejectors: These generate high force using explosive cartridges. They are single-use and can produce significant shock loads.
- Pneumatic Ejectors: These separate the store using compressed air. They are clean and fast but typically generate lower force.
- Hydraulic/Electromechanical Ejectors: These provide controlled force and are reusable, but their systems are more complex [6].
- In the selection of an appropriate ejector system, several factors should be considered, including the type and mass of the store, the characteristics of the carrier aircraft and the mission profile.

#### 1.3.2.2 Types of ejectors and their characteristics

There are some criteria should be considered when determining the ejector force. First

- The force must be sufficient to minimize the store's release duration.
- Excessive force may lead to store instability.
- The distribution of force between the forward and aft ejectors is important to ensure that the store follows the desired trajectory [6].

MIL-HDBK-244A includes the following statement regarding the distribution of ejector forces: "Typical ejector force distribution should be biased forward to ensure pitch-down rotation during release" [6].

Numerical simulations are widely used to analyze the effects of ejector forces on the store. In particular, six degrees of freedom (6-DOF) simulations allow detailed modeling of the store's motion during separation [7].

Selecting the appropriate ejector system is critical to ensure the store separates safely and stably from the aircraft. In determining the ejector type and force levels, the characteristics of the store, flight conditions, and mission profile must be considered. Moreover, numerical simulations should be employed to analyze the effects of different ejector force profiles on the store, and the most suitable ejector configuration should be identified.

The ejector selection and ideal force-aft force distribution for this study will be detailed in the Eglin Test Case Validation section. Figure 1.2 shows an example of the time-dependent variation of the force applied by the ejector [8]. In actual applications, the force applied to the store changes over time as shown in the figure until the store fully separates from the aircraft. However, in the Eglin test case, this is not the case. In the published data, a constant force is applied to the store until the ejector reaches its stroke length—i.e., just before the store separates from the aircraft. Once the maximum stroke length is exceeded, the force applied by the ejector to the store drops to zero.

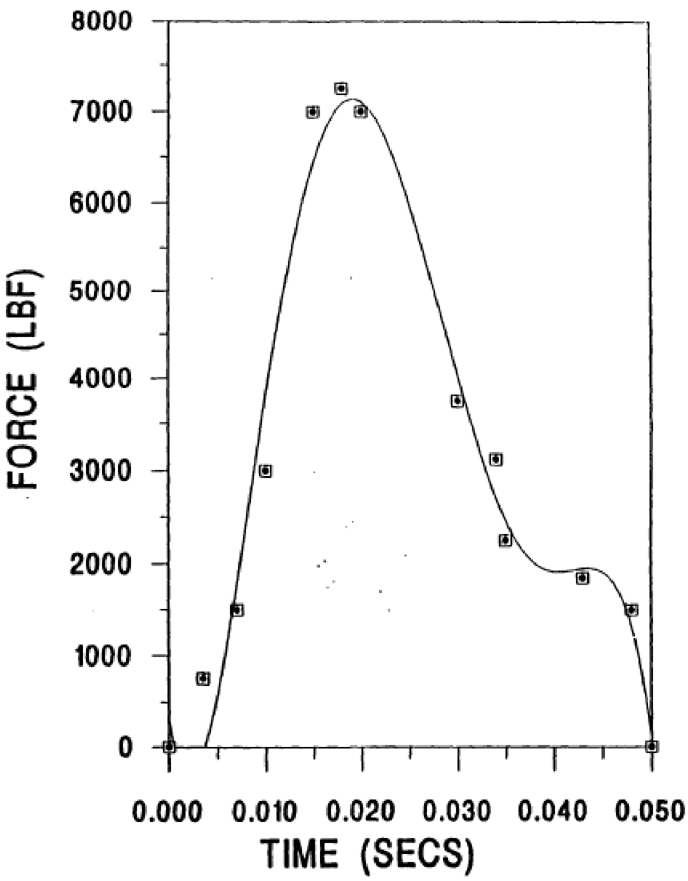


**Figure 1.2 :** An example for ejector force distribution with respect to time

### 1.3.3 Carrying – release envelope for stores

Store carriage and separation envelopes define critical parameters for the safe transport and release of stores in fighter aircraft and other aerial vehicles. These envelopes encompass the aerodynamic configuration of the store, flight conditions, carriage position, and the dynamic effects at the moment of release. A properly designed store separation envelope ensures both the structural integrity of the carrier aircraft and the smooth, controlled release of the store from the aircraft. Figure 3 shows the store carriage and release envelopes for a particular aircraft [9]. Due to the scarcity of information on this topic in the literature, this study will consider the carriage and release envelopes depicted in Figure 1.3.

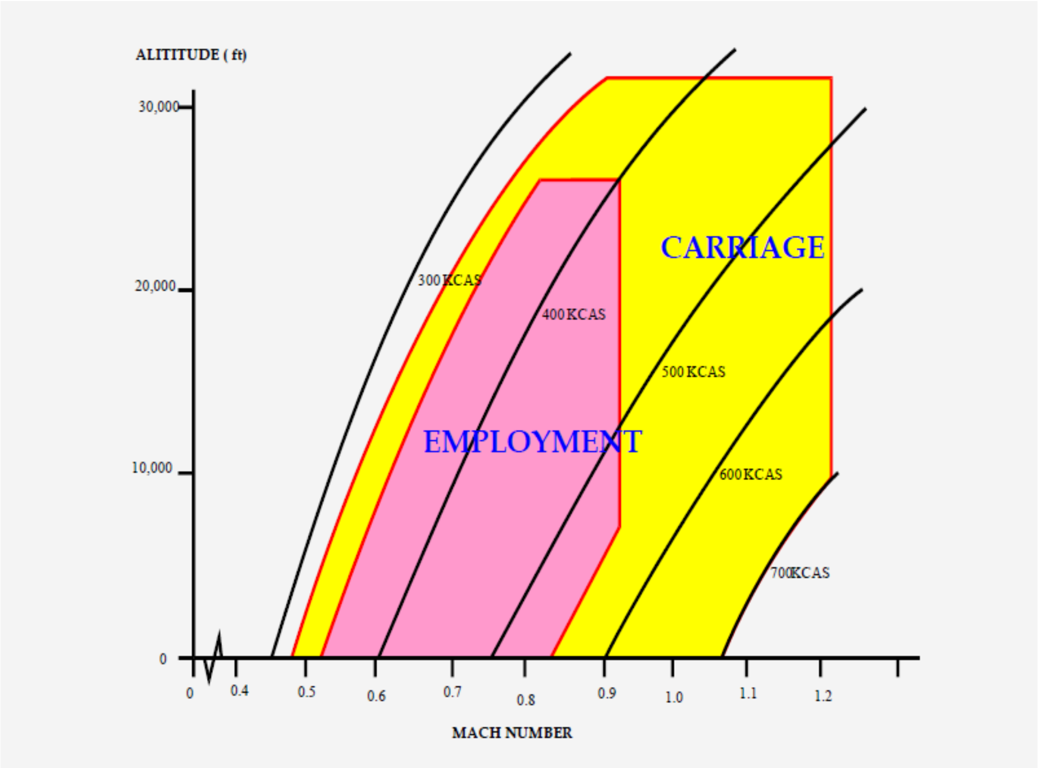


**Figure 1.3 :** An example of store carriage and release envelope

### 1.4 An important assumption for separation analysis

In order to perform separation analysis, aerodynamic data of the store under launch conditions is required. For this purpose, CFD data provided by TUSAŞ has been used. This data was obtained in the form of a grid dataset by using the geometries of the Generic 5th Generation Fighter Aircraft and the Eglin Pylon-Store, which are available in open sources, in CFD simulations. This data is solely applicable for equations of motion the store.

To enable separation analysis under different flight conditions and aircraft maneuvers, a 6-DOF model of the aircraft must be developed, and aerodynamic data for this model is needed. Since such data is not available for the aircraft used in the CFD geometry, existing data from the literature for the F-16 is used. Therefore, in this study, separation analyses were performed using the flight dynamics of the F-16 aircraft and a store moving within the flow field of the Generic 5th Generation Fighter geometry.

## 2. STORE MATHEMATICAL MODELLING

Same equations of motion are applicable for both store in free flight and aircraft, because same physical principles drive motion of both. Whereas relative motion of store with respect to aircraft necessitates some updates on the conventional flight dynamics reference frames, coordinate systems, motion variables and nomenclature. Mathematical modeling of store separation can be considered as 2 sequential phases based on the store motion relative to the aircraft. In the first phase, the store is carried by the aircraft so the store and the aircraft move together as a single body. During the second phase, the store interacts with the aircraft and moves relative to the aircraft. In the beginning of this phase, the store is under the effects of aerodynamic loads and ejector forces. After the ejector stroke length reached, ejector forces become zero, only aerodynamic loads effect the store. From now on, the store is in free flight and moves relative to the aircraft under the effect of the nonuniform flow field. This phase continues until the uniform flow field begins where far enough from aircraft.

The separation process begins with the instant of release. So, the second phase will be our concern for mathematical modeling. The first phase only determines the initial conditions of the store motion relative to the aircraft. In this work ejector parameters of the Eglin Test case [2] will be used. The end-of-stroke conditions form the initial conditions for the free flight phase. Store separation equations of motions are derived from “Store Separation Equations of Motion” article [10].

## 2.1 Store Frames

### 2.1.1 Aircraft body axis

The aircraft axis is closely related to the conventional aircraft body axis encountered in flight Dynamics literature (the directions are aligned; only the points of origin are different). The aircraft reference frame rotates to maintain constant orientation with respect to the aircraft at all times. Aircraft axis can be seen in Figure 2.1.

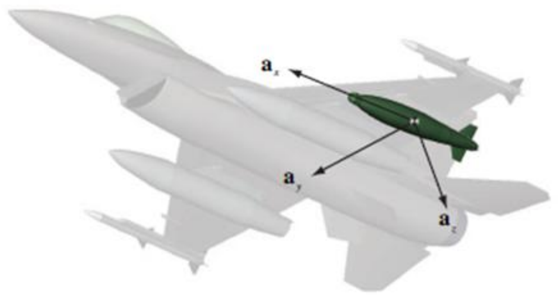


**Figure 2.1 :** Definition of aircraft axis coordinate system

### 2.1.2 Store body axis

The origin of the store body axis, OB, is determined by the store CG, which may in principle change during the trajectory (due to changing configurations or burning propellant). The bx direction is aligned with the centerline of the store and positive out of the nose. The bz direction is perpendicular to bx and positive downward. The by direction is determined by by = bz × bx and by consequence is positive out of the starboard side of the store. The body axis is oriented with respect to the aircraft axis by the installed incidence angles. The store body axis is shown graphically in Figure 2.2.

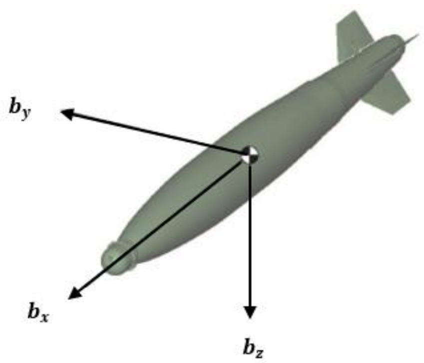


**Figure 2.2 :** Definition of store body axis coordinate system

### 2.1.3 Earth axis

For typical flight vehicle navigation equations, the north-east-down directions with reference to the latitude and longitude of the vehicle determine the earth axis directions. However, for store separation, a local approximation is sufficient. Implicit in this approximation is the assumption of a flat earth. The earth axis origin OE is defined as the store CG at the moment of release. The origin is fixed in space relative to the surface of the earth. The primary direction of interest for the earth axis is the local vertical ez, which defines the orientation of the gravity vector. The vector ey is perpendicular to ez and is positive out of the right wing of the aircraft (starboard) as seen by the pilot. The vector ex is defined by the cross-product ex = ey × ez and by consequence lies in the local horizontal plane positive in the forward direction as seen by the pilot.

### 2.1.4 Inertial axis

The choice of an inertial reference frame is of crucial importance for dynamics problems in general and flight mechanics problems in particular. An inertial reference frame is adequately described as a reference frame at rest with respect to the distant stars. In many flight vehicle applications, the earth itself can serve as a suitable reference frame. In store separation analysis, a further approximation is warranted. The inertial reference frame is selected as a hypothetical frame moving at a constant translational velocity relative to the earth, where the velocity and orientation of the frame are determined by the aircraft flight axis velocity and orientation at the instant the store is released. This provides an important advantage of referencing the inertial motion of the store and the aircraft to the same inertial reference frame and provides a convenient way to describe the relative motion between the store and aircraft. In the limiting case of straight and level flight during release, the aircraft itself becomes a suitable inertial reference frame and the store motion relative to the aircraft is directly obtained. For more general aircraft maneuvers, a transformation is straightforward using the common inertial reference frame. The origin of the inertial axis, OI, is coincident with the store CG at the moment of release and travels in a straight line with a constant velocity equal to the velocity of the flight axis at the instant of release.

### 2.1.5 Flight axis

The flight axis is defined by the direction of the aircraft velocity vector throughout the trajectory. The flight axis is coincident with the inertial axis at the instant of release, but translates and rotates relative to the inertial axis as the aircraft velocity vector changes. For steady flight conditions, the flight axis and inertial axis remain coincident throughout the trajectory. The origin of the flight axis, OF, is defined as a point coincident with the store CG at the moment of release but is fixed relative to the aircraft and thus translates along with the aircraft during the maneuver. Aircraft body axis, Store Body axis, Earth Axis, Inertial Axis and Flight Axis are shown in Figure 2.3.

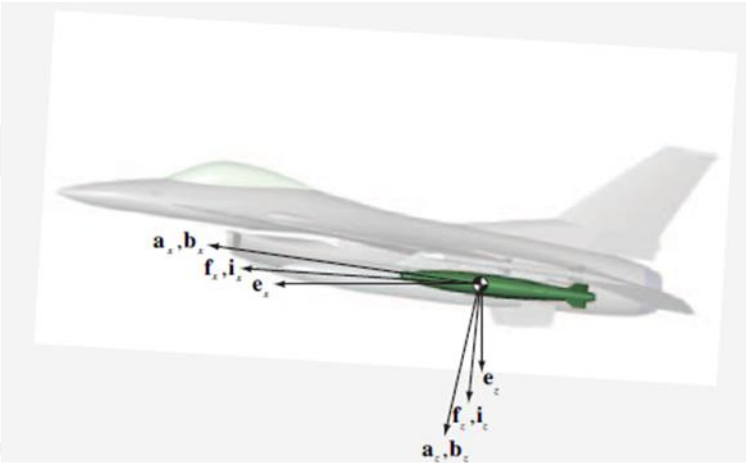


**Figure 2.3 :** Definition of earth, inertial and flight axes

Figure 2.4 shows the positions of the axes at the moment of release and after some time. As seen, the Earth axis remains at the store's CG position at the moment of release, while the Inertial axis continues to move with the velocity vector at release. The Aircraft body axis is oriented according to the aircraft's attitude relative to the ground, and the Flight axis changes direction based on the aircraft's velocity vector. Finally, the Store body axis undergoes changes in position and orientation due to the aerodynamic and inertial loads acting on it.

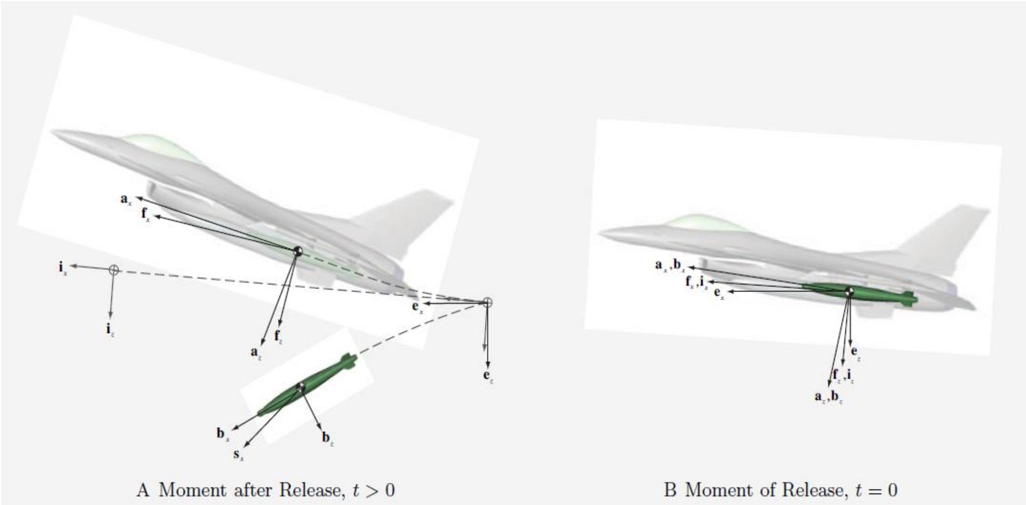


**Figure 2.4 :** Axis positions at moments of release and a moment after release

### 2.1.6 Atmospheric wind axis

For the purposes of store separation, the atmospheric winds surrounding the aircraft at release are assumed to be monolithic (uniform) and moving at a constant velocity relative to the surface of the earth. The particular velocity of the wind is rarely important since only the motion of the store relative to the wind and relative to the aircraft is of interest. The monolithic assumption allows the wind to be modeled as an idealized rigid body and represented by a reference frame. The assumed constant translational velocity also qualifies the atmospheric wind frame as a suitable inertial reference frame, a fact that will be useful in deriving the so-called wind axis equations of motion. The atmospheric wind axis W{wx,wy,wz} is aligned with the earth axis E{ex, ey, ez} with the origin of the atmospheric wind axis OW moving at a constant velocity relative to the origin of the earth axis OE, where the magnitude of the velocity is defined by the atmospheric winds. If the atmospheric winds are assumed to be identically zero, then the atmospheric wind axis and earth axis are coincident.

### 2.1.7 Store wind axis

The Store Wind Axis S{sx, sy, sz} is established in the Store Wind Reference Frame. The store wind axis is quite different from the previously defined atmospheric wind axis. The origin of the store wind axis OS is coincident with the store CG throughout the trajectory. The velocity of the store relative to the local wind reference frame determines the orientation of the store wind axis. The velocity and orientation of the store wind axis with respect to the atmospheric wind axis is essential for determining the aerodynamic forces acting on the store during flight. The sx direction rotates to maintain alignment with the store velocity vector. The sz direction is perpendicular to sx and positive in the downward direction. The sy direction is defined by sy = sz ×sx. The store wind axis is shown graphically in Figure 2.5.

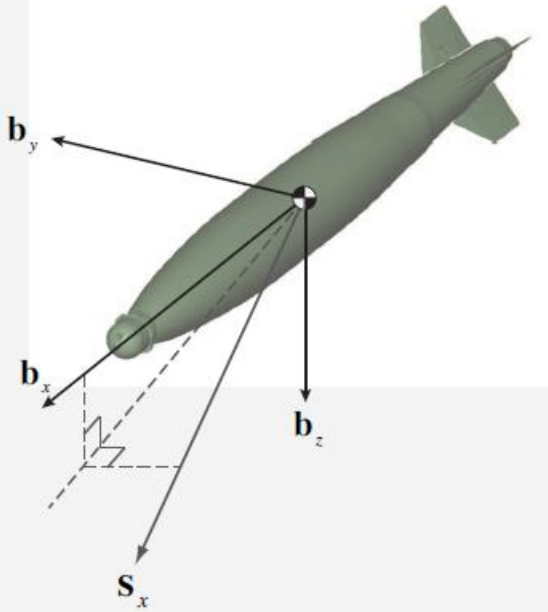


**Figure 2.5 :** Store body axis and store wind axis

The frames described above are generally used in typical store separation scenarios. In these scenarios, some assumptions are made to simplify the separation process. For example, since only straight and level flight is considered, the inertial frame is defined by assuming that the aircraft maintains the velocity and attitude it had at the moment of release. Also, because the aircraft's orientation and velocity are assumed not to change after release, the atmospheric wind frame is not used. However, in this study, the inertial frame will not be used. Instead, the store's motion will be defined relative to the ground rather than the inertial frame. The aircraft's motion will also be defined relative to the ground, and the positional and angular motions of both relative to each other will be considered to assess safe separation. Moreover, the aircraft's motion will not be limited to straight flight but will be extended to include various maneuvers. Therefore, defining an inertial frame will not meet the requirements of this study.

## 2.2 Store separation equation of motions

Store separation equations of motions are very similar to the conventional aircraft equations of motion. Literature includes many sources about equation of motions. For this study equations of motions are derived by using [10]. These equations of motion apply to both the aircraft and the store. While deriving the equations of motion, the motions of the aircraft and the store relative to the ground were calculated first, and then the relative position and orientation differences between the aircraft and the store were determined. Equations of motions are given in Equation 1-12.

### 2.2.1 Translational dynamics

$$\dot{u} = F_x/m \; - gsin\theta - qw + rv \tag{2.1}$$

$$\dot{v} = F_y/m \; + gcos\theta sin\phi + pw - ru \tag{2.2}$$

$$\dot{w} = F_z/m \; + gcos\theta cos\phi - pv + qu \tag{2.3}$$

### 2.2.2 Rotational kinematics

$$\dot{\phi} = p + \tan\theta\,(q\sin\phi + r\cos\phi) \tag{2.4}$$

$$\dot{\theta} = q\cos\phi - r\sin\phi \tag{2.5}$$

$$\dot{\psi} = (q\sin\phi + r\cos\phi)\sec\theta \tag{2.6}$$

### 2.2.3 Rotational dynamics

$$\dot{p} = (I_{xx}I_{zz} - I_{xz}^2)^{-1}\,[\left(I_{xz}M_z + I_{zz}M_x + \left(I_{yy}I_{zz} - I_{xz}^2 - I_{zz}^2\right)qr + \left(I_{xx}I_{xz} - I_{xz}I_{yy} + I_{xz}I_{zz}\right)pq\right] \tag{2.7}$$

$$\dot{q} = I_{yy}^{-1}\,[M_y + I_{xz}(r^2 - p^2) + pr\,(I_{zz} - I_{xx})] \tag{2.8}$$

$$\dot{r} = (I_{xx}I_{zz} - I_{xz}^2)^{-1}\,[\left(I_{xz}M_x + I_{xx}M_z + \left(I_{xz}I_{yy} - I_{xx}I_{xz} - I_{xz}I_{zz}\right)qr + \left(I_{xx}^2 + I_{xz}^2 - I_{xx}I_{yy}\right)pq\right] \tag{2.9}$$

### 2.2.4 Translational kinematics

$$\dot{x} = u\cos\theta\cos\psi - \mathrm{v}\,(\sin\phi\sin\theta\cos\psi - \cos\phi\sin\psi) + \mathrm{w}\,(\cos\phi\sin\theta\cos\psi + \sin\phi\sin\psi) \tag{2.10}$$

$$\dot{y} = u\cos\theta\sin\psi + \mathrm{v}(\sin\phi\sin\theta\sin\psi + \cos\phi\cos\psi) + \mathrm{w}(\cos\phi\sin\theta\sin\psi - \sin\phi\cos\psi] \tag{2.11}$$

$$\dot{z} = -u\sin\theta + v\sin\phi\cos\theta + w\cos\phi\cos\theta \tag{2.12}$$

## 2.3 Store 6-Dof Simulink Model

A 6-DOF simulation is required to calculate the position and attitude information of the store at each time step. The model setup is based on the reference [11] where a Boeing 747 was modeled. For the store modeling, the aerodynamic database was updated, thrust effects were set to zero, and ejector effects were added.

### 2.3.1 Aerodynamic model

Aerodynamic force and moment coefficients were input into the model as time series by reading data tables from the Eglin test case. Additionally, the dynamic moment coefficients (Cl_p, Cm_q, Cn_r) provided in the Eglin report were integrated into the aerodynamic model.

In Chapter 6, the aerodynamic database will be updated with grid data analyses involving a fifth-generation fighter aircraft and Eglin stores, so the structure here will change accordingly.

### 2.3.2 Ejector model

In the literature review section, ejector types and mechanism explained. Then, a typical ejector force distribution with respect to time were shared. In separation analyses of stores, the variation of ejector forces over time often follows a pattern similar to the one shown in this example. However, there are also cases where the ejector forces remain constant over time. In the Eglin test case analysis, the ejector force profile does not vary with time. The Eglin separation analysis report [2] indicates that once the store moves away from the aircraft by the ejector stroke length, its connection with the ejector is severed and the applied forces drop to zero. In this study ejector forces and moments considered as constant until the store reaches the stroke length, after which they drop to zero. In the Eglin test case, forces of 2400 lbf and 9600 lbf are applied at the front and rear ejector points, respectively. These values will be preserved in the model validation section, Chapter 3. Then, same force distribution of front and rear ejector will be used in the safe separation scenarios described in Section 6.

# 3. STORE 6-DOF MODEL VALIDATION

In the experimental study of store separation problems, the Eglin Store Separation Test Series conducted by the United States Air Force is one of the most comprehensive and widely referenced works in the aerospace literature. These tests were carried out by the USAF SEEK EAGLE Office (AFSEO) operating at Eglin Air Force Base in Florida. The primary objective of the Eglin test series is to investigate the dynamic behaviors that occur during the separation of stores from high-speed fighter aircraft in various configurations and to validate the safety of these separation processes. The tests observed risks such as collisions, deviations, and loss of control that threaten the structural integrity of both the store and the carrier platform.

The tests were generally conducted on F-4 Phantom and F-16 Fighting Falcon aircraft, with separated stores including general-purpose bombs like the MK-82 and MK-84 as well as AGM-series guided missiles.

Figure 3.1 shows the Eglin test setup. As seen, a symmetric dual wing-pylon and store geometry is present. While the wings are kept fixed, the store is moved to the next position using a sting.

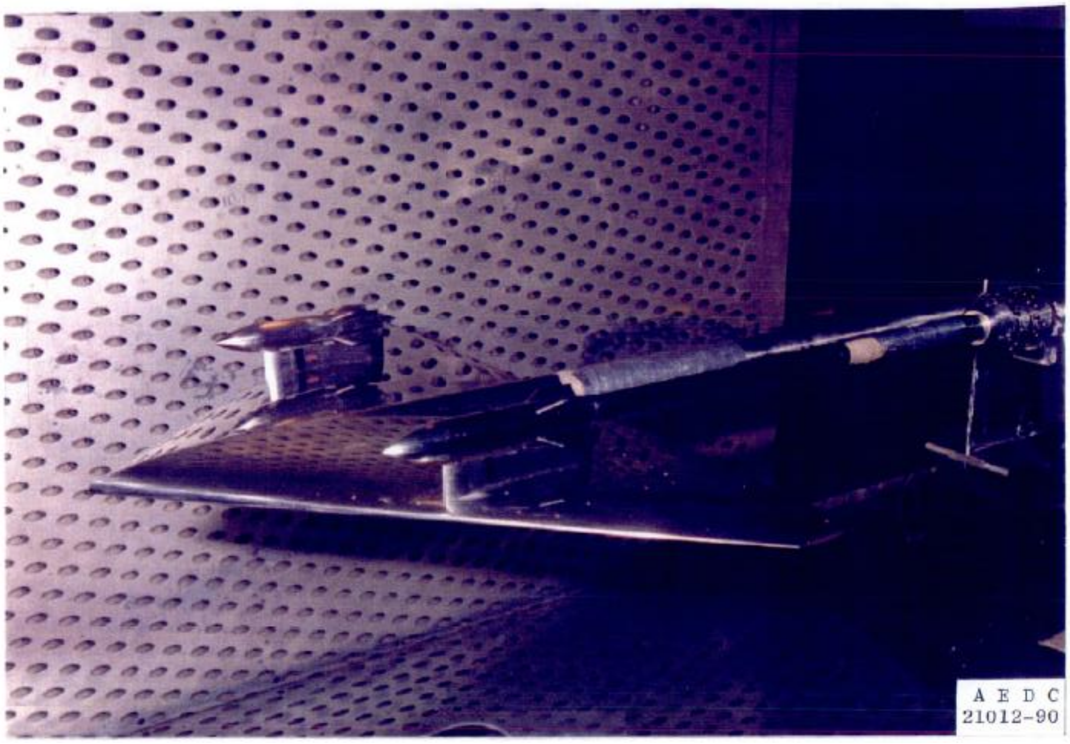


**Figure 3.1 :** Eglin test setup

Table 3.1 shows the data for the store and other elements of the test setup as presented in the Eglin document [2]. These data will be used to validate the Eglin test case and subsequently to conduct safe separation scenarios.

**Table 3.1 :** Full scale store and ejector characteristics.

| Properties | Explanation | Value | Unit |
|---|---|---|---|
| Weight | Weight | 2000 | lbf |
| X_CG | Center of Gravity | 4.65 | ft |
| Ixx | Roll Moment of Inertia | 20 | slug/ft2 |
| Iyy | Pitch Moment of Inertia | 360 | slug/ft2 |
| Izz | Yaw Moment of Inertia | 360 | slug/ft2 |
| CLP | Roll Damping Coefficients | -4 | 1/rad |
| CMQ | Pitch Damping Coefficients | -40 | 1/rad |
| CNR | Yaw Damping Coefficients | -40 | 1/rad |
| X_FE | Forward Ejector Location | 4.06 | ft |
| X_AE | Aft ward Ejector Location | 5.73 | ft |
| Stroke Length | Ejector Stroke Length | 0.33 | ft |

### 3.1 Eglin Geometry

Figure 3.2 shows the store along with the sting that holds the store under the aircraft and moves it to the next position in the following time step. Note that the units are in inches. Figure 3.3 also shows the wing and pylon geometries together with the store.

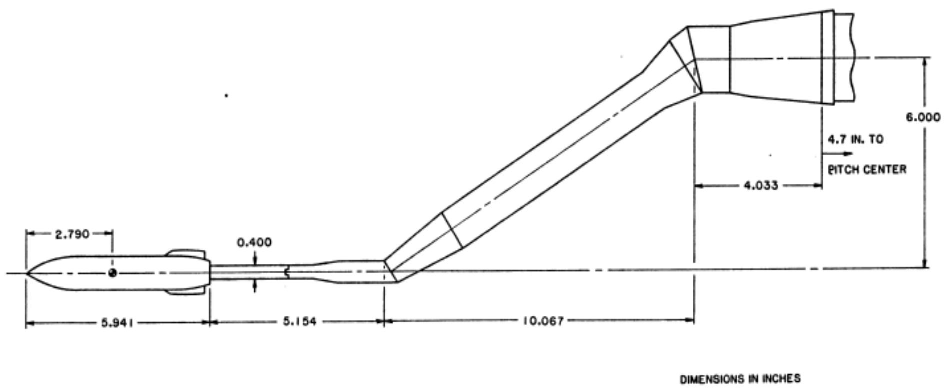


**Figure 3.2 :** Store with sting in wind tunnel test section

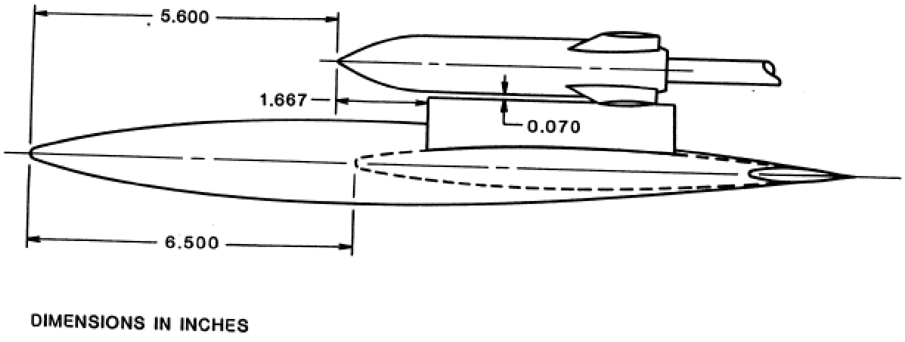


**Figure 3.3 :** Eglin wing-pylon-store geometry

### 3.2 Eglin Test Results

The aerodynamic data and store trajectory were obtained using the CTS (Captive Trajectory System) method. The CTS method is explained in Section 1.3.1. In the Eglin test result report, velocities, attitude angles, positions, rates, ejector forces and the aerodynamic forces that the store is exposed to up to the safe separation distance are given in a table. Since size of this table data is massive, it will be shared under two headings.

The 6-DOF simulation model takes the aerodynamic force and moment coefficients and ejector forces from here as time series inputs and calculates the store's velocity, position, rates, acceleration, and attitude information at each time step. In the last step, calculated parameters and table data are compared to validate the 6 DOF model.

#### 3.2.1 Aerodynamic data and ejector force data

The aerodynamic data and store trajectory were obtained using the CTS (Captive Trajectory System) method. The CTS method is explained in Section 1.3.1. Aerodynamic force and moment coefficient and ejector forces of forward and aft ejector values at each time step are shown in Table 3.2. Test data are in timeseries format and it continues until 0.33 second with 0.01 second time step.

**Table 3.2 :** Aerodynamic data and ejector forces data of Eglin test case.

| T(s) | CN | CLM | CY | CLN | CLL | CAT | FE1(lbf) | FE2(lbf) |
|---|---|---|---|---|---|---|---|---|
| 0.000 | 0.00 | 0.00 | 0.00 | 0.00 | 0.00 | 0.00 | 2400 | 9600 |
| 0.010 | 0.00 | 0.00 | 0.01 | 0.02 | 0.05 | 0.00 | 2400 | 9600 |
| 0.020 | 0.00 | 0.00 | 0.04 | 0.08 | 0.20 | 0.10 | 2400 | 9600 |
| 0.030 | -0.01 | -0.01 | 0.10 | 0.19 | 0.45 | 0.20 | 2400 | 9600 |
| 0.040 | -0.01 | -0.01 | 0.17 | 0.34 | 0.80 | 0.30 | 2400 | 9600 |
| 0.050 | -0.02 | -0.02 | 0.27 | 0.52 | 1.26 | 0.50 | 2400 | 9600 |
| 0.060 | -0.03 | -0.03 | 0.38 | 0.75 | 1.78 | 0.70 | 0 | 0 |
| 0.070 | -0.04 | -0.04 | 0.50 | 1.01 | 2.28 | 0.80 | 0 | 0 |
| 0.080 | -0.05 | -0.05 | 0.62 | 1.30 | 2.73 | 1.00 | 0 | 0 |
| 0.090 | -0.06 | -0.06 | 0.74 | 1.62 | 3.16 | 1.20 | 0 | 0 |
| 0.100 | -0.07 | -0.07 | 0.87 | 1.97 | 3.54 | 1.40 | 0 | 0 |
| 0.110 | -0.09 | -0.09 | 0.99 | 2.34 | 3.89 | 1.60 | 0 | 0 |
| 0.120 | -0.10 | -0.10 | 1.12 | 2.73 | 4.20 | 1.80 | 0 | 0 |
| 0.130 | -0.12 | -0.12 | 1.25 | 3.14 | 4.48 | 2.00 | 0 | 0 |
| 0.140 | -0.14 | -0.13 | 1.38 | 3.57 | 4.71 | 2.20 | 0 | 0 |
| 0.150 | -0.16 | -0.14 | 1.51 | 4.02 | 4.91 | 2.40 | 0 | 0 |
| 0.160 | -0.18 | -0.16 | 1.64 | 4.48 | 5.07 | 2.60 | 0 | 0 |
| 0.170 | -0.21 | -0.17 | 1.78 | 4.95 | 5.20 | 2.80 | 0 | 0 |
| 0.180 | -0.24 | -0.19 | 1.91 | 5.44 | 5.28 | 3.00 | 0 | 0 |
| 0.190 | -0.26 | -0.20 | 2.05 | 5.94 | 5.32 | 3.30 | 0 | 0 |
| 0.200 | -0.29 | -0.22 | 2.19 | 6.43 | 5.33 | 3.50 | 0 | 0 |
| 0.210 | -0.32 | -0.23 | 2.33 | 6.94 | 5.29 | 3.70 | 0 | 0 |
| 0.220 | -0.36 | -0.24 | 2.48 | 7.44 | 5.22 | 4.00 | 0 | 0 |
| 0.230 | -0.39 | -0.26 | 2.62 | 7.94 | 5.10 | 4.20 | 0 | 0 |
| 0.240 | -0.43 | -0.27 | 2.77 | 8.43 | 4.95 | 4.40 | 0 | 0 |
| 0.250 | -0.46 | -0.28 | 2.91 | 8.92 | 4.75 | 4.70 | 0 | 0 |
| 0.260 | -0.50 | -0.29 | 3.06 | 9.40 | 4.52 | 4.90 | 0 | 0 |
| 0.270 | -0.54 | -0.29 | 3.21 | 9.87 | 4.24 | 5.20 | 0 | 0 |
| 0.280 | -0.59 | -0.30 | 3.36 | 10.32 | 3.92 | 5.40 | 0 | 0 |
| 0.290 | -0.63 | -0.30 | 3.51 | 10.77 | 3.56 | 5.60 | 0 | 0 |
| 0.300 | -0.68 | -0.31 | 3.67 | 11.19 | 3.17 | 5.90 | 0 | 0 |
| 0.310 | -0.73 | -0.31 | 3.83 | 11.61 | 2.74 | 6.10 | 0 | 0 |
| 0.320 | -0.78 | -0.31 | 3.98 | 12.01 | 2.27 | 6.30 | 0 | 0 |
| 0.330 | -0.83 | -0.31 | 4.14 | 12.39 | 1.77 | 6.50 | 0 | 0 |

### 3.2.2 Store trajectory data

Eglin test results includes store movement parameters from release moment throughout separation process. Table 3.3 shows position and attitude angles of the store at each time step. Test process ends at 0.33 second. Because store reaches to safe distance from carrier aircraft in Z axis.

**Table 3.3 :** Position and attitude angles of store in Eglin test case.

| T(s) | X(ft) | Y(ft) | Z(ft) | $\psi$(deg) | $\theta$(deg) | $\phi$(deg) |
|---|---|---|---|---|---|---|
| 0.000 | 0.00 | 0.00 | 0.00 | 0.00 | 0.00 | 0.00 |
| 0.010 | 0.00 | 0.00 | 0.01 | 0.02 | 0.05 | 0.00 |
| 0.020 | 0.00 | 0.00 | 0.04 | 0.08 | 0.20 | 0.10 |
| 0.030 | -0.01 | -0.01 | 0.10 | 0.19 | 0.45 | 0.20 |
| 0.040 | -0.01 | -0.01 | 0.17 | 0.34 | 0.80 | 0.30 |
| 0.050 | -0.02 | -0.02 | 0.27 | 0.52 | 1.26 | 0.50 |
| 0.060 | -0.03 | -0.03 | 0.38 | 0.75 | 1.78 | 0.70 |
| 0.070 | -0.04 | -0.04 | 0.50 | 1.01 | 2.28 | 0.80 |
| 0.080 | -0.05 | -0.05 | 0.62 | 1.30 | 2.73 | 1.00 |
| 0.090 | -0.06 | -0.06 | 0.74 | 1.62 | 3.16 | 1.20 |
| 0.100 | -0.07 | -0.07 | 0.87 | 1.97 | 3.54 | 1.40 |
| 0.110 | -0.09 | -0.09 | 0.99 | 2.34 | 3.89 | 1.60 |
| 0.120 | -0.10 | -0.10 | 1.12 | 2.73 | 4.20 | 1.80 |
| 0.130 | -0.12 | -0.12 | 1.25 | 3.14 | 4.48 | 2.00 |
| 0.140 | -0.14 | -0.13 | 1.38 | 3.57 | 4.71 | 2.20 |
| 0.150 | -0.16 | -0.14 | 1.51 | 4.02 | 4.91 | 2.40 |
| 0.160 | -0.18 | -0.16 | 1.64 | 4.48 | 5.07 | 2.60 |
| 0.170 | -0.21 | -0.17 | 1.78 | 4.95 | 5.20 | 2.80 |
| 0.180 | -0.24 | -0.19 | 1.91 | 5.44 | 5.28 | 3.00 |
| 0.190 | -0.26 | -0.20 | 2.05 | 5.94 | 5.32 | 3.30 |
| 0.200 | -0.29 | -0.22 | 2.19 | 6.43 | 5.33 | 3.50 |
| 0.210 | -0.32 | -0.23 | 2.33 | 6.94 | 5.29 | 3.70 |
| 0.220 | -0.36 | -0.24 | 2.48 | 7.44 | 5.22 | 4.00 |
| 0.230 | -0.39 | -0.26 | 2.62 | 7.94 | 5.10 | 4.20 |
| 0.240 | -0.43 | -0.27 | 2.77 | 8.43 | 4.95 | 4.40 |
| 0.250 | -0.46 | -0.28 | 2.91 | 8.92 | 4.75 | 4.70 |
| 0.260 | -0.50 | -0.29 | 3.06 | 9.40 | 4.52 | 4.90 |
| 0.270 | -0.54 | -0.29 | 3.21 | 9.87 | 4.24 | 5.20 |
| 0.280 | -0.59 | -0.30 | 3.36 | 10.32 | 3.92 | 5.40 |
| 0.290 | -0.63 | -0.30 | 3.51 | 10.77 | 3.56 | 5.60 |
| 0.300 | -0.68 | -0.31 | 3.67 | 11.19 | 3.17 | 5.90 |
| 0.310 | -0.73 | -0.31 | 3.83 | 11.61 | 2.74 | 6.10 |
| 0.320 | -0.78 | -0.31 | 3.98 | 12.01 | 2.27 | 6.30 |
| 0.330 | -0.83 | -0.31 | 4.14 | 12.39 | 1.77 | 6.50 |

Store velocity and angular rates data in Eglin test result report is shown in Table 3.4. These velocity values are given in inertial frame. Therefore 6 DOF model results will be calculated in inertial frame. Then Eglin test results and 6 DOF model results will be compared.

**Table 3.4 :** Velocity and angular rate data of store in Eglin test case.

| T(s) | U(ft) | V(ft) | W(ft) | P(rad/s) | Q(rad/s) | R(rad/s) |
|---|---|---|---|---|---|---|
| 0.000 | 0.0 | 0.0 | 0.0 | 0.00 | 0.00 | 0.00 |
| 0.010 | -0.2 | -0.2 | 2.1 | 0.08 | 0.18 | 0.07 |
| 0.020 | -0.3 | -0.3 | 4.3 | 0.17 | 0.35 | 0.15 |
| 0.030 | -0.5 | -0.5 | 6.4 | 0.22 | 0.52 | 0.22 |
| 0.040 | -0.7 | -0.6 | 8.5 | 0.25 | 0.70 | 0.29 |
| 0.050 | -0.9 | -0.7 | 10.7 | 0.27 | 0.88 | 0.35 |
| 0.060 | -1.2 | -0.8 | 11.7 | 0.29 | 0.90 | 0.41 |
| 0.070 | -1.5 | -0.9 | 11.9 | 0.29 | 0.84 | 0.47 |
| 0.080 | -1.7 | -0.9 | 12.0 | 0.29 | 0.78 | 0.52 |
| 0.090 | -2.0 | -0.9 | 12.2 | 0.29 | 0.72 | 0.57 |
| 0.100 | -2.2 | -0.9 | 12.4 | 0.29 | 0.66 | 0.61 |
| 0.110 | -2.5 | -0.9 | 12.5 | 0.30 | 0.59 | 0.65 |
| 0.120 | -2.7 | -0.9 | 12.7 | 0.30 | 0.53 | 0.68 |
| 0.130 | -3.0 | -0.9 | 12.8 | 0.30 | 0.47 | 0.72 |
| 0.140 | -3.2 | -0.9 | 13.0 | 0.30 | 0.41 | 0.75 |
| 0.150 | -3.4 | -0.8 | 13.1 | 0.30 | 0.35 | 0.78 |
| 0.160 | -3.6 | -0.7 | 13.2 | 0.30 | 0.29 | 0.8 |
| 0.170 | -3.8 | -0.6 | 13.3 | 0.31 | 0.22 | 0.83 |
| 0.180 | -4.1 | -0.5 | 13.5 | 0.31 | 0.16 | 0.85 |
| 0.190 | -4.2 | -0.4 | 13.6 | 0.32 | 0.09 | 0.86 |
| 0.200 | -4.4 | -0.2 | 13.7 | 0.32 | 0.03 | 0.87 |
| 0.210 | -4.6 | 0.0 | 13.8 | 0.33 | -0.04 | 0.88 |
| 0.220 | -4.8 | 0.2 | 14.0 | 0.34 | -0.10 | 0.88 |
| 0.230 | -4.9 | 0.4 | 14.1 | 0.35 | -0.17 | 0.88 |
| 0.240 | -5.0 | 0.6 | 14.2 | 0.35 | -0.24 | 0.88 |
| 0.250 | -5.2 | 0.8 | 14.4 | 0.35 | -0.31 | 0.87 |
| 0.260 | -5.3 | 1.1 | 14.5 | 0.35 | -0.38 | 0.86 |
| 0.270 | -5.4 | 1.4 | 14.6 | 0.35 | -0.45 | 0.85 |
| 0.280 | -5.5 | 1.7 | 14.8 | 0.36 | -0.51 | 0.84 |
| 0.290 | -5.5 | 2.0 | 14.9 | 0.36 | -0.58 | 0.82 |
| 0.300 | -5.6 | 2.3 | 15.1 | 0.35 | -0.64 | 0.81 |
| 0.310 | -5.6 | 2.6 | 15.3 | 0.35 | -0.71 | 0.79 |
| 0.320 | -5.6 | 2.9 | 15.5 | 0.35 | -0.77 | 0.77 |
| 0.330 | -5.6 | 3.2 | 15.7 | 0.34 | -0.83 | 0.76 |

## 3.3 Validation

As a result of validating the developed 6-DOF model with the Eglin data, the simulation and tabular data are shown in Figure 3.4 [2]. As can be seen, the simulation results closely follow the trends of the tabular data. This indicates that the simulation is functioning correctly and is suitable for the next steps.

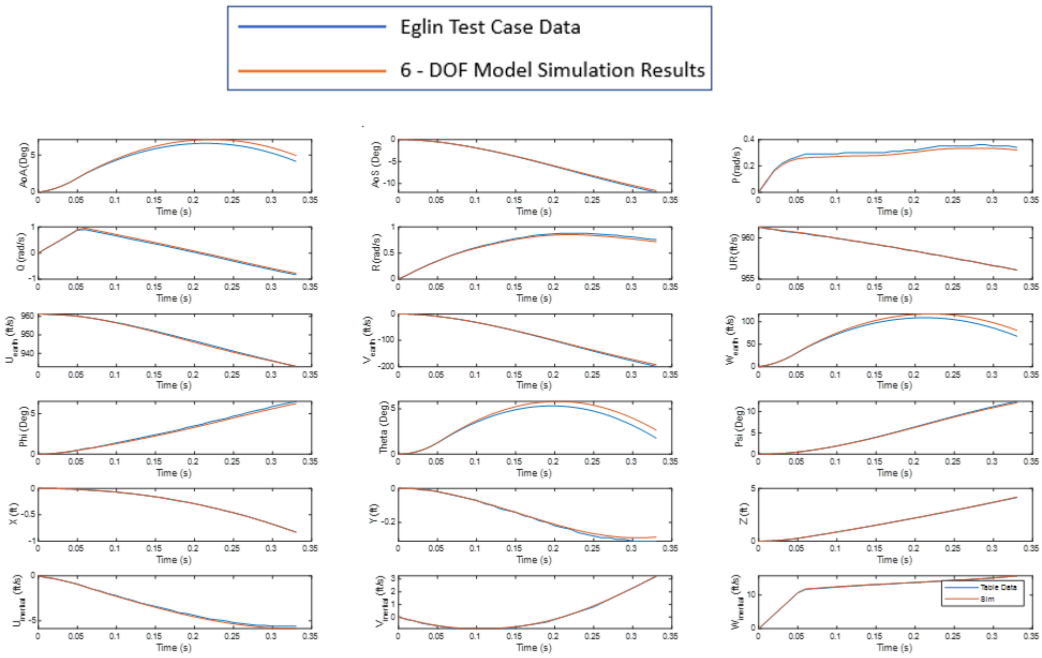


**Figure 3.4 :** Comparison of simulation results and experimental CTS data

# 4. GENERIC FIFTH GENERATION FIGHTER AIRCRAFT

Store separation analyses are planned to be conducted using the model validated with the Eglin data. For this purpose, aerodynamic analyses of the store under the aircraft during different flight conditions are required. To this end, a fifth-generation fighter aircraft model similar to the F-22 available in the literature has been used.

This aircraft model is an open-source platform that resembles the geometry of the F-22 and replicates its aerodynamic characteristics. It provides researchers with a foundation to perform development and validation activities in their own studies.

The SSAM-Gen5 model is based on the F-22 Raptor and is presented in Figure 4.1. This vehicle was chosen over the F-35 as the majority of in-service fifth-generation vehicles have a twin-engine configuration. The geometry was generated from drawings and images of the aircraft that are openly available on the public domain. As such, the geometry is not intended to reproduce the aerodynamic characteristics of the F-22 Raptor, but rather, to reflect the salient aerodynamic features typical of contemporary aircraft. The geometry can be downloaded from [12].

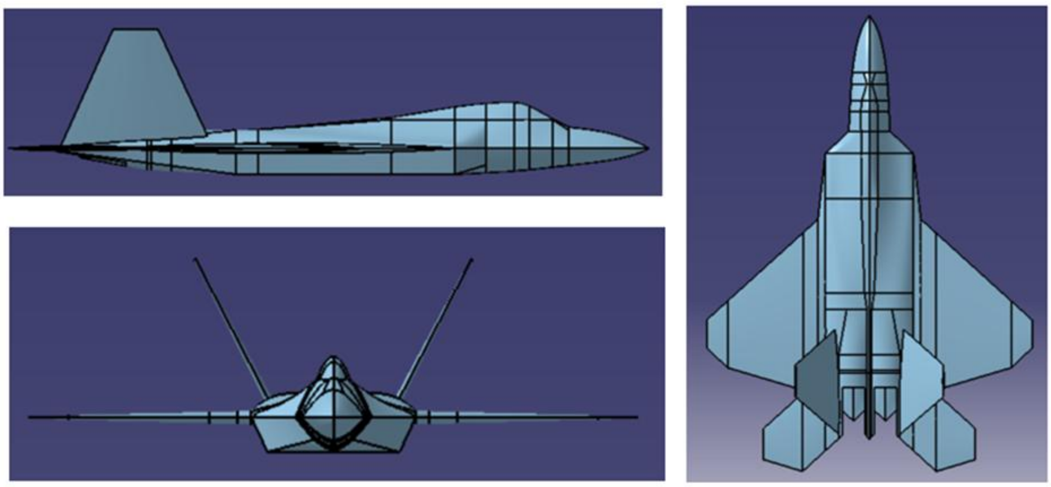

**Figure 4.1 :** Fifth generation high performance aircraft

## 4.1 Grid Data

In section 1.4. assumption for the aerodynamic data source of safe separation analysis used in this study was explained. The Generic Fifth Generation Fighter Aircraft described in Chapter 4 was integrated with the Eglin store and pylon, and CFD analyses were conducted. As a result of these analyses, grid data was obtained. The breakpoints of the grid data are shown in Table 4.1. The grid data were generated through CFD analyses performed using open-source geometries by Turkish Aerospace Industries (TAI/TUSAŞ).

**Table 4.1 :** Store grid data breakpoints.

| Breakpoint | Value |
|---|---|
| Mach | 0.8, 0.9 |
| X (ft) | -15, -6.3, -3.4, -2, -1.1, -0.5, 0, 0.25, 0.44, 0.725, 1.2, 2.15, 5 |
| Y (ft) | -5, -2.3, -1.4, -1, -0.7, -0.5, 0, 0.5, 0.7, 1, 1.4, 2.3, 5 |
| Z (ft) | 0, 0.4, 1, 2, 4, 10 |
| Theta (deg) | -20, -10, 0, 10 |
| AoA (deg) | 0, 5, 10 |

# 5. F-16 MODEL – TRIM PROCESS

In the literature, most store separation scenarios are conducted under level flight conditions. In this case, the aircraft continues straight and level flight after releasing the store. To simplify this scenario, an inertial frame is defined for the aircraft. The inertial frame is explained in Chapter 2.1.4. According to this definition, the inertial frame coincides with the store's center of gravity until the moment of release, and they move together. From the instant the store is released, it moves at a constant velocity equal to the aircraft's velocity vector at the release moment. The instantaneous position and attitude of the store relative to this frame are calculated for collision checks. This approach eliminates the need for a 6-DOF model of the aircraft.

In this study, not only level flight but also firings during pull-up and coordinated turn maneuvers will be tested. During these firings, it will be checked whether the store collides with the aircraft. Therefore, to perform a flight simulation, a 6-DOF aircraft model is required. For this reason, an F-16 model with aerodynamic and engine data available in the literature has been preferred and developed [13]. This F-16 model has been trimmed for various conditions, and these trim conditions are used as initial states for the simulations. The resulting aircraft position and attitude data from these simulations will be used in the Store Separation section.

## 5.1 F-16 Model

In the literature, there is an important document titled "Simulator study of stall/post-stall characteristics of a fighter airplane with relaxed longitudinal static stability" [13], which contains published aerodynamic and engine data related to the F-16. Researchers who aim to develop an F-16 model typically use this document as a reference to build their models. The document titled Nonlinear F-16 Model Description [14] extensively explains the modeling of the F-16 aircraft using the data from this reference. In this study, the F-16 model was established based on the information in these documents. Since aircraft modeling is not the main focus of this work, further details will not be discussed here. The air-related parameters of the F-16 are shown in Table 5.1 [14]. Control surface limits are shown in Table 6.2 [14].

**Table 5.1 :** F-16 mass and inertia data.

| Parameter | Symbol | Value | Unit |
|---|---|---|---|
| Aircraft Mass | M | 636.9427 | slug |
| Reference Wing Span | B | 30 | ft |
| Reference Wing Area | S | 300 | $ft^2$ |
| Mean Aerodynamic Chord | $\bar{c}$ | 11.32 | ft |
| Roll Moment of Inertia | $I_{xx}$ | 9496 | $slug.ft^2$ |
| Pitch Moment of Inertia | $I_{yy}$ | 55814 | $slug.ft^2$ |
| Yaw Moment of Inertia | $I_{zz}$ | 63100 | $slug.ft^2$ |
| Product Moment of Inertia | $I_{xz}$ | 982 | $slug.ft^2$ |
| Product Moment of Inertia | $I_{xy}$ | 0 | $slug.ft^2$ |
| Product Moment of Inertia | $I_{yz}$ | 0 | $slug.ft^2$ |
| CG Location | $x_{cg}$ | $0.3\bar{c}$_ | ft |
| Reference CG Location | $x_{cg_r}$ | $0.35\,\bar{c}$ | ft |

**Table 5.2 :** Control surface limits.

| Control | Units | Min | Max |
|---|---|---|---|
| Throttle | - | 0 | 100 |
| Elevator | deg | -25 | 25 |
| Ailerons | deg | -21.5 | 21.5 |
| Rudder | deg | -30 | 30 |
| Leading Edge Flaps | deg | 0 | 25 |

### 5.2 Trim

In the literature, most of the store separation analysis conducted under level flight conditions. For this scenario inertial frame assumption is sufficient.

In this study safe separation in various flight conditions are reviewed. To achieve this, it is necessary to demonstrate that the aircraft can fly with the store under the given flight condition. This requires trimming the aircraft while carrying the store for that specific flight condition. For this purpose, a trim algorithm was developed based on the paper titled “A General Solution to the Aircraft Trim Problem” [15]. Using this trim algorithm and the F-16 model, trim solutions were obtained for various flight conditions. These trim points will serve as initial conditions for the store separation simulations.

Since trim is not the main focus of this study, detailed explanations about trim codes will not be provided here.

### 5.2.1 Trim assumptions

Trim analysis conducted by making some assumptions to avoid modelling and trim complexities. Assumptions listed below:

- The weight, inertia, and aerodynamic effects of the store were not included in the aircraft's trim conditions during trim calculation.
- For the reason above, after the store is released, the store's effect on the aircraft was not removed. The aircraft did not experience any change in weight or aerodynamic force/moment after releasing the store.
- The release conditions of the store directly adopt the aircraft's trim conditions. The rates at the aircraft's center of gravity (CG) were not transferred to the store's CG.

### 5.2.2 Trim conditions

Trim was performed at different Mach numbers and altitudes for various flight conditions such as Level Flight, Climb, Descent, Pull-Up, and Coordinated Turn maneuvers. The trim variables determined for each flight condition are shown in the Table 5.3.

**Table 5.3 :** Trim conditions.

| Trim Condition | Mach | Altitude (kft) | Gama (Deg) | Phi (Deg) | Nz (g) |
|---|---|---|---|---|---|
| Descent | 0.8, 0.9 | 10, 20 | -10, -5 | 0 | 0 |
| Cruise | 0.8, 0.9 | 10, 20 | 0 | 0 | 0 |
| Climb | 0.8, 0.9 | 10, 20 | 10, 5 | 0 | 0 |
| Pull-Up | 0.8, 0.9 | 10, 20 | 0 | 0 | 2-7 |
| Coordinated Turn | 0.8, 0.9 | 10, 20 | 0 | 15, 30, 45, 60, 75 | 0 |

# 6. SEPARATION ANALYSIS

Up to this point in the study, the following steps have been completed: The F-16 fighter aircraft was trimmed for various flight conditions, and then simulations were run using these trim conditions as initial conditions for both the aircraft and the store. The instantaneous position and attitude information of the aircraft and the store relative to the ground were obtained. At this stage, to examine the relative motion between the aircraft and the store, the CAT models of both were imported into MATLAB in STL format. The MATLAB figure showing the aircraft and the store together is presented in Figure 6.1.

Reminder: The F-16 model was used for trim and aircraft simulation, while generic fighter and Eglin geometries were used for the grid data.

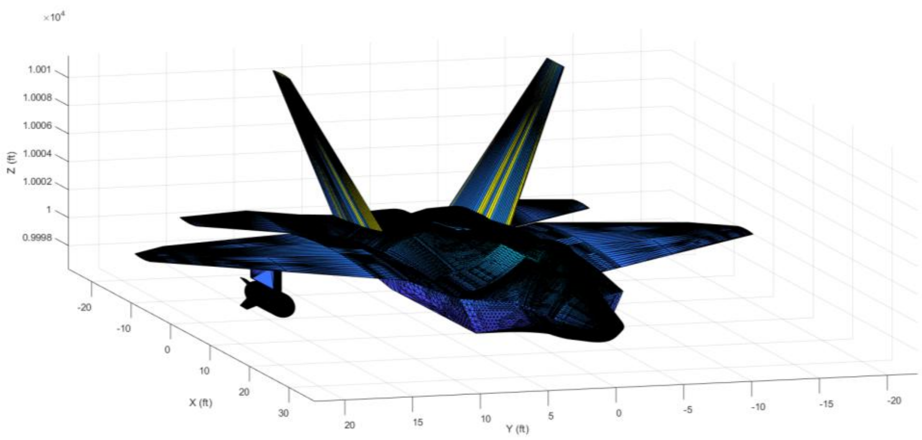


**Figure 6.1 :** Aircraft and store graphic before release

Then, using the positions and attitudes of the aircraft and store at each time step, they were visually represented on the graphics. Examples for different flight conditions can be seen in Figure 6.2-6.6.

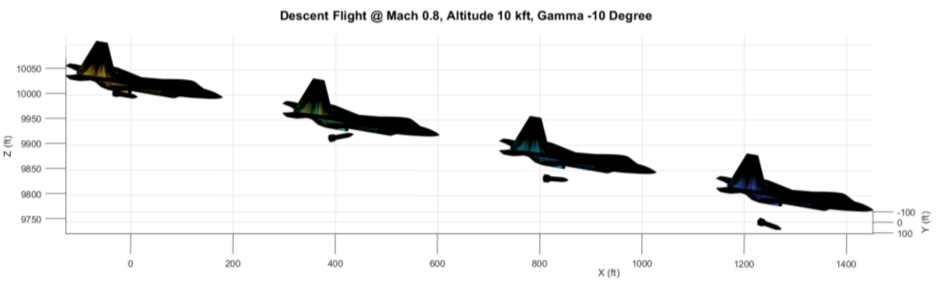


**Figure 6.2 :** Descent flight store separation

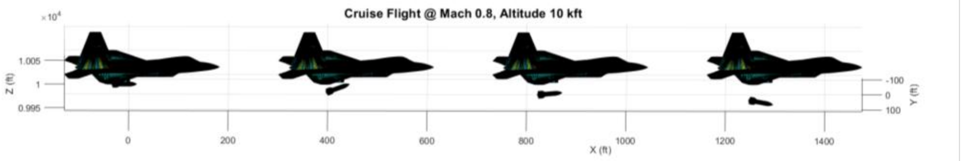


**Figure 6.3 :** Cruise flight store separation

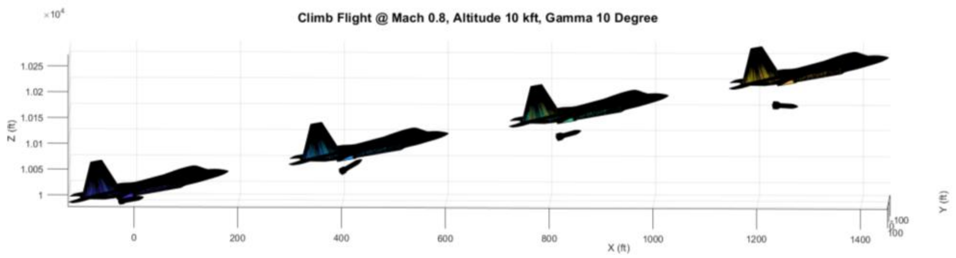


**Figure 6.4 :** Climb flight store separation

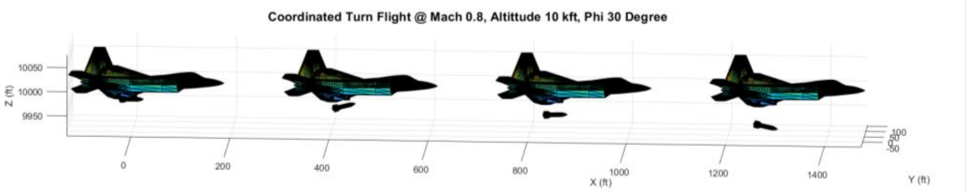


**Figure 6.5 :** Coordinated turn maneuver store separation

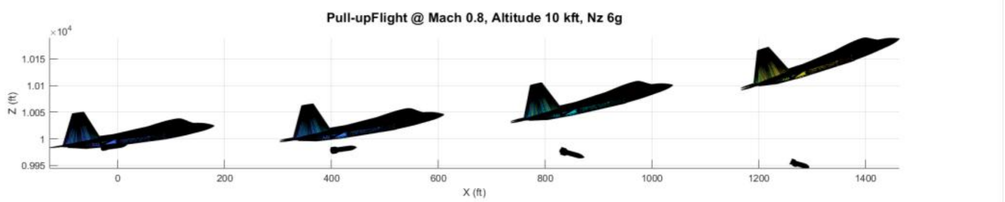


**Figure 6.6 :** Pull-Up maneuver store separation

The aircraft and store are scaled up by a factor of 5 in these visuals, with images captured every 1 seconds to create the graphics. The total simulation duration is 3 seconds, as safe separation is considered achieved once the store has moved at least 10 meters (≈ 32 feet) away from the aircraft. Store separation primarily involves the release and ejection of a store while it is still within the aircraft's flow field, which typically extends about 20 to 30 feet from the original carriage location (Cenko, 1991).

## 6.1 Box Analysis Method

It is possible to perform collision tests using the STL files of the aircraft and the store. However, STL files contain a large number of triangles, and checking for collisions between each pair of triangles significantly increases computation time. Instead, a more efficient approach is to determine the smallest rectangular boxes that enclose the aircraft and the store, and then check for overlaps between these boxes at each time step. For this purpose, rectangular boxes have been defined for both the aircraft and the store. The rectangular box defined for the aircraft is shown in Figure 6.7.

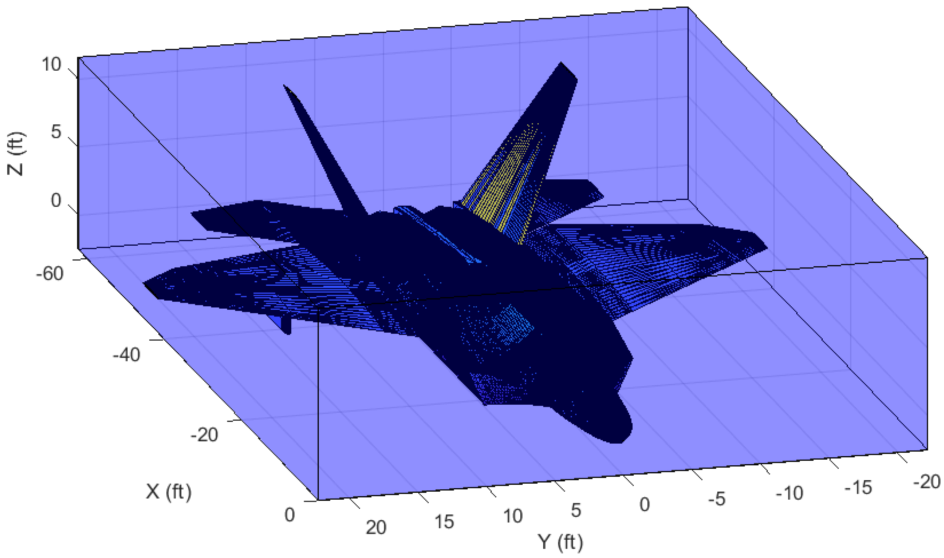


**Figure 6.7 :** Box determination for whole aircraft

Since the rectangular box defined for the aircraft was considered too conservative, the aircraft was divided into parts as shown below, and boxes were defined for each part. This approach also facilitates collision checking for each external component on the aircraft. When there is additional equipment such as other stores, landing gears, fuel

tanks, etc., separate boxes can be defined for each, and it becomes very practical to test for overlaps between these boxes and the store's box at every time step.
The aircraft with all its parts together and their corresponding boxes defined is shown in Figure 6.8. Figure 6.9 also shows each part separately.

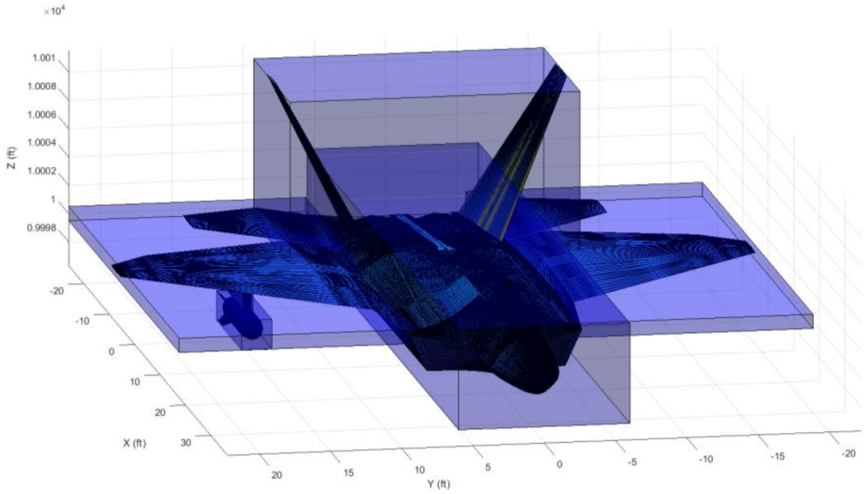


**Figure 6.8 :** Box determination for aircraft parts

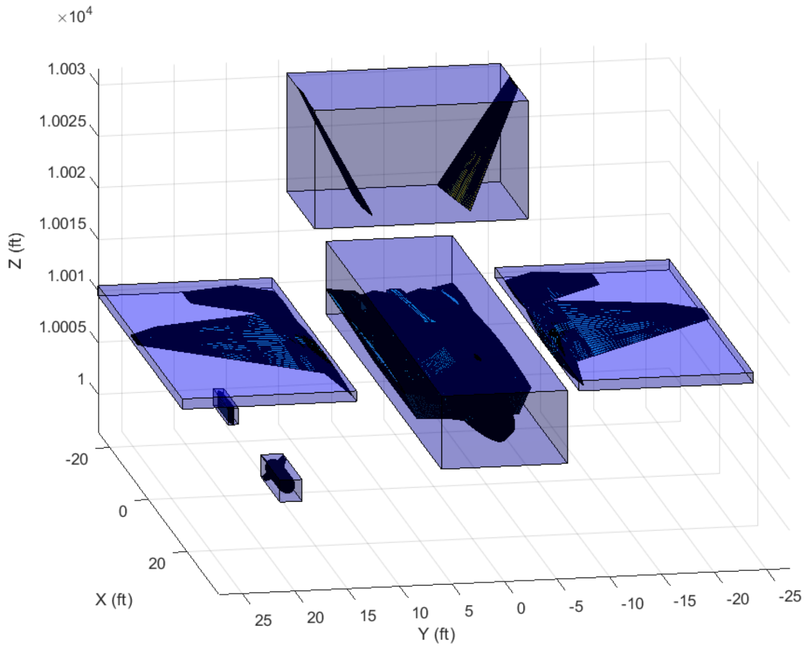


**Figure 6.9 :** Box determination for aircraft parts (separated demonstration)

The boxes drawn for the separation analyses can be multiplied by certain safety factors to increase the minimum required clearance distance between the store and the aircraft. There are multiple methods to verify that these boxes do not collide at each time step:

### 6.1.1 Axis-aligned bounding box (AABB) method

In store separation analyses, various geometric collision detection methods are used to quickly and practically determine whether the released store risks colliding with the carrier aircraft. One such method is the Axis-Aligned Bounding Box (AABB). AABB defines rectangular volumes (boxes) aligned with the coordinate axes that encompass the geometries of the store and aircraft, allowing collision checks through simple axis comparisons [16].

The AABB method is especially useful in 6 Degrees of Freedom (6-DOF) simulations to determine whether the store comes into contact with the aircraft or other stores at any time during its trajectory. It is computationally efficient compared to complex surface collision calculations. AABBs are typically recalculated and updated at every simulation step to perform collision checks [17].

Advantages of AABB in store separation studies can be summarized as follows:

- Provides collision detection with low computational load suitable for real-time simulations.
- Allows simplified volumetric analysis without requiring the complex geometry of the aircraft or store.
- Particularly effective in preliminary assessments and defining safe separation envelopes.

However, since the AABB method only considers axis-aligned overlaps, it can introduce errors when the store rotates. In such cases, more advanced methods like Oriented Bounding Box (OBB) or exact mesh-mesh collision checks may be preferred [18].

Since the store and aircraft undergo both translational and rotational motion during separation, AABB is not suitable.

### 6.1.2 Separated axis theorem (SAT)

In computational geometry and physics-based simulations, the Separated Axis Theorem (SAT) is a fundamental method used for collision detection between convex shapes. The principle of SAT states that if two convex objects are not intersecting, there exists at least one axis along which the projections of the two objects do not overlap [19].

In store separation simulations, especially those involving high-fidelity geometry models and relative motions between the aircraft and the store, SAT provides a more accurate alternative to simpler bounding methods like Axis-Aligned Bounding Boxes (AABB). Since the store and aircraft can rotate and move non-linearly, SAT offers an advantage by allowing checks on axes that are aligned with the shapes' orientation—not just the global coordinate system [17].

SAT is particularly useful when:

- The geometry of the store or aircraft is approximated using convex polygons or polyhedral.
- Accurate collision detection is required, especially under dynamic motion and orientation.
- Store trajectories include significant pitch, yaw, or roll rotations that make axis-aligned bounding boxes insufficient [16].

The basic idea involves:

- Generating a set of potential separating axes, typically the normal to the faces of each convex shape and the cross products of edge pairs.
- Projecting both shapes onto each axis.
- Checking for overlapping intervals. If there is an axis on which the intervals do not overlap, then the objects are not colliding [17].

Despite its higher computational cost compared to AABB, SAT provides better precision, which is critical in applications such as missile and bomb release analysis where precise clearance verification is required between the store and the aircraft structure.

Therefore, in this study, collision checking between the boxes has been performed using the Separated Axis Theorem.

# 7. RESULTS AND DISCUSSIONS

Trim conditions for separation analysis were mentioned in Chapter 5.2.2. A total of 4 cruise, 8 climb, 8 descent, 20 coordinated turn, and 24 pull-up trim conditions (Totally 80) were computed, followed by their respective simulations. The store was also simulated using the initial conditions obtained from the trim results. The relative position and orientation of the store and the aircraft were evaluated based on their motions with respect to the ground. Using the Separated Axis Theorem, the intersection of the bounding boxes assigned to the store and the aircraft was checked, and in almost all cases, safe separation was observed.

Although variables such as the magnitude and distribution of the ejector forces (front and rear), flight speed, and altitude have the potential to prevent safe separation, no such risk was observed in the analyses performed. With further analyses, all scenarios in which safe separation occurs or fails could be identified. However, for the scope of this thesis, the current level of analysis is considered sufficient.

Some of the results of the store separation analyses are shown in the following sections.

## 7.1 Descent, Climb and Cruise Flight Separation Graphics

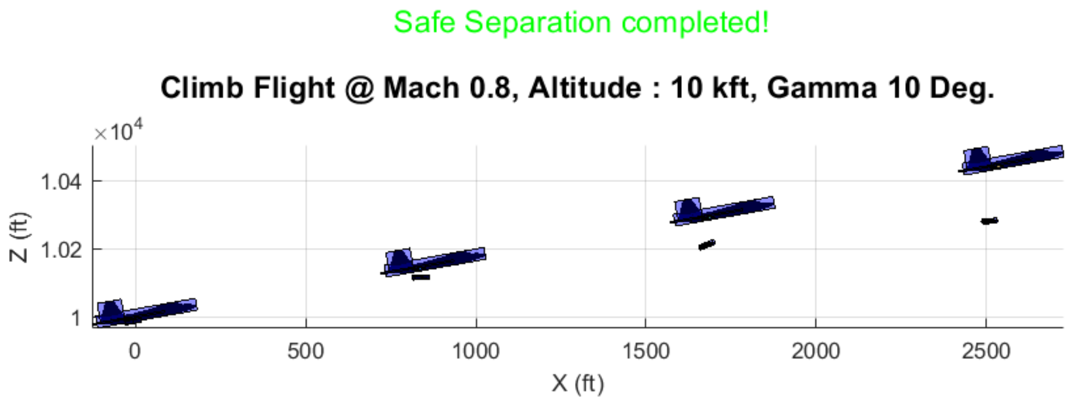


**Figure 7.1 :** Climb Flight @Mach 0.8, Alt 10 Kft, Gamma 10 Degree

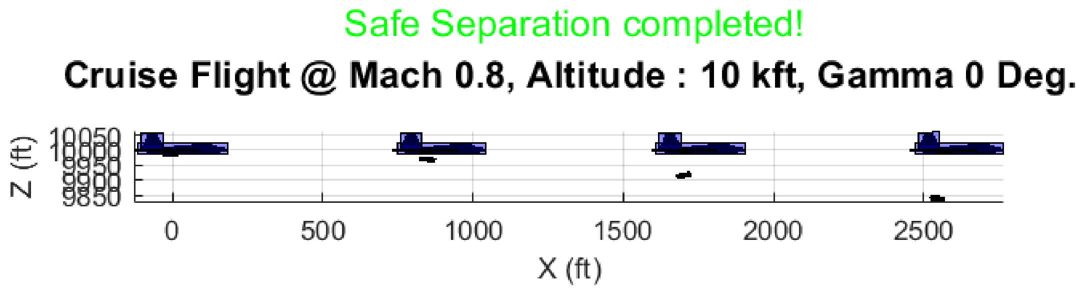


**Figure 7.2 :** Cruise Flight @Mach 0.8, Alt 10 Kft, Gamma 0 Degree

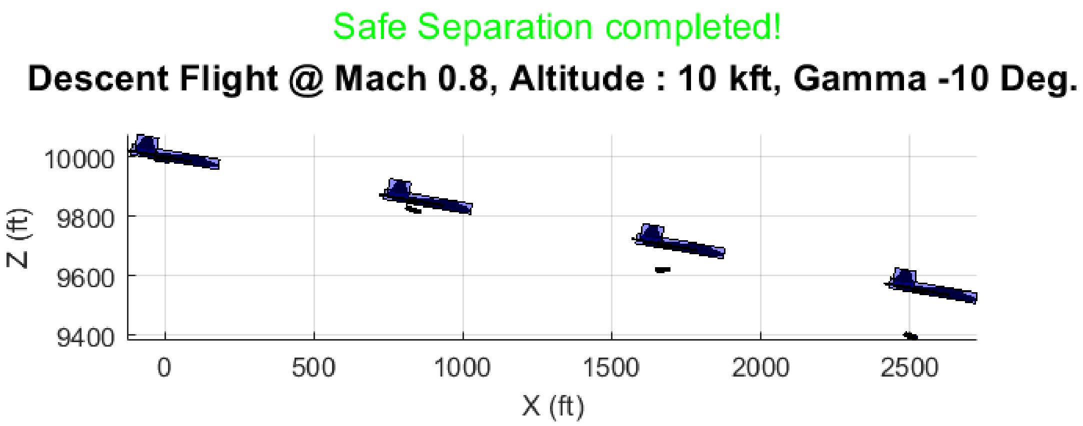


**Figure 7.3 :** Descent Flight @Mach 0.8, Alt 10 kft, Gamma -10 Degree

## 7.2 Coordinated Turn Maneuver Separation Graphics

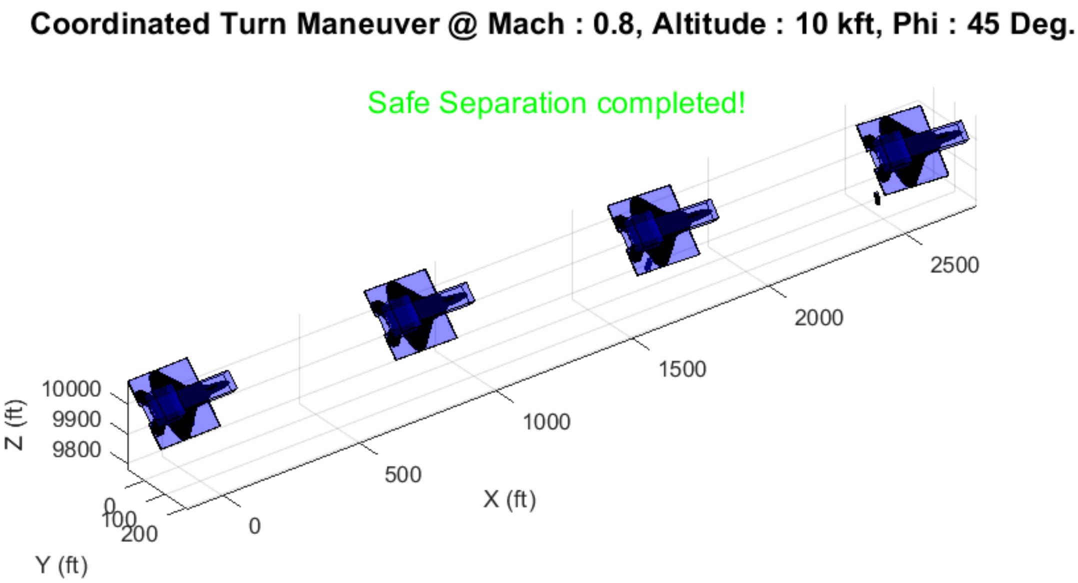


**Figure 7.4 :** Coord. Turn Maneuver @Mach 0.8, Alt 10 kft, Phi 45 Deg.

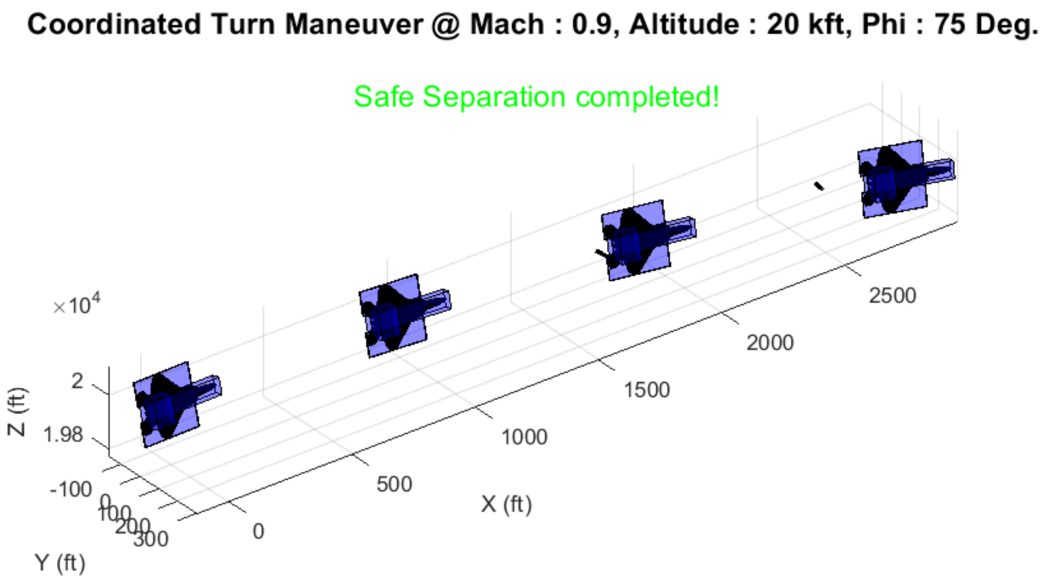


**Figure 7.5 :** Coord. Turn Maneuver @Mach 0.9, Alt 20 kft, Phi 75 Deg.

### 7.3 Pull-Up Maneuver Separation Graphics

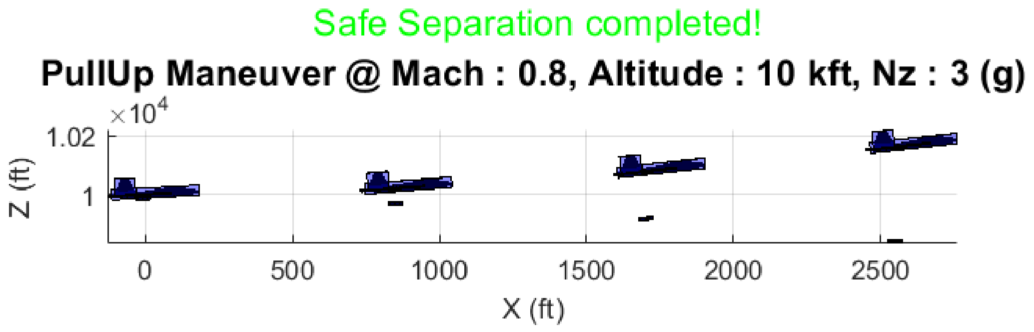


**Figure 7.6 :** Pull-Up Maneuver @Mach 0.8, Alt 10 kft, Nz 3 (g)

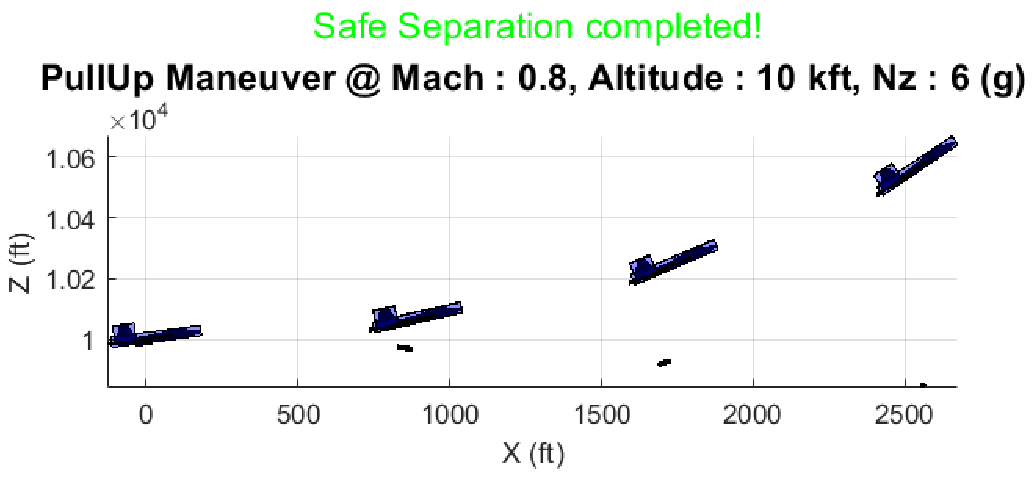


**Figure 7.7 :** Pull-Up Maneuver @Mach 0.8, Alt 10 kft, Nz 6 (g)

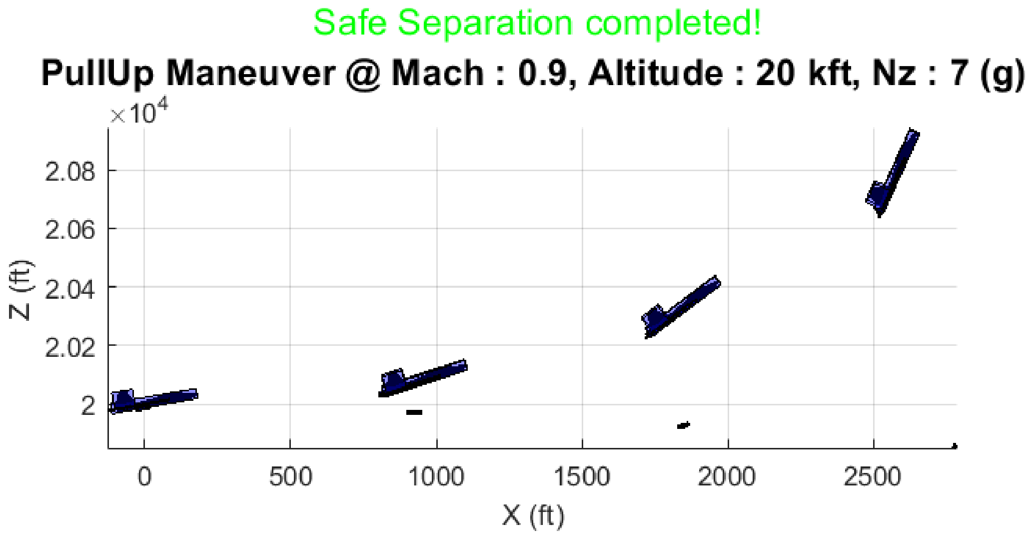


**Figure 7.8 :** Pull-Up Maneuver @Mach 0.9, Alt 20 kft, Nz 7 (g)

## 7.4 Recommendations for Future Works

As future work, incorporating the effect of the store during aircraft trim and reflecting the influence of store separation on the subsequent motion of the aircraft in the simulation will be of particular importance. Additionally, store release from internal stations is another critical topic that needs to be investigated. Since cavity flow involves unsteady aerodynamic phenomena, separation analysis from internal bays will require significantly more effort compared to external store release.

# REFERENCES


[1] **Cook, M. V.** (2007). Flight Dynamics Principles: A Linear Systems Approach to Aircraft Stability and Control. Butterworth-Heinemann.

[2] **Heim, E. R. (1991)** CFD Wing/Pylon/Finned Store Mutual Interference Wind Tunnel Experiment, Calspan Corporation/AEDC Operations, Final Report for Period September 1-17,1990

[3] **Prashanth, R. K., Sucheendran, M. M.** (2014). "Store Separation Analysis Using Computational Fluid Dynamics." *IRF International Conference, 30th March-2014, Pune, India, ISBN: 978-93-82702-69-6*

[4] **Peters, Nicholas & Wissink, Andrew & Ekaterinaris, John.** (2023). Machine learning-based surrogate modeling approaches for fixed-wing store separation. Aerospace Science and Technology. 133. 108150. 10.1016/j.ast.2023.108150.

[5] **Osman, A. A., Aly, A. M., Khalil, E. E., & Abdelattif, O. E.** (2016, January). *Numerical analysis of an external store separation from an airplane* (AIAA Paper No. 2016-2143). In AIAA Modeling and Simulation Technologies Conference. American Institute of Aeronautics and Astronautics.https://doi.org/10.2514/6.2016-2143.

[6] MIL-HDBK-244A: Guidance for Aircraft Stores Compatibility. U.S. Department of Defense.

[7] **Etkin, B., & Reid, L. D.** (1996). Dynamics of Flight: Stability and Control (3rd ed.). Wiley.

[8] **Hansen, D. M. (2001).** *Store separation methodology analysis* (Master's thesis, Air Force Institute of Technology). Defense Technical Information Center (DTIC). https://apps.dtic.mil/sti/tr/pdf/ADA245148.pdf

[9] NATO Science and Technology Organization. (2018). *Store Separation Overview: Educational notes* (STO-EN-SCI-277). NATO STO. https://www.sto.nato.int/publications/STO%20Educational%20Notes/STO-EN-SCI-277-2018/EN-SCI-277-2018-04.pdf

[10] **Carter. R. E.** (2012) Store Separation Equations of Motion, AIAA Atmospheric Flight Mechanics Conference 13 - 16 August 2012, Minneapolis, Minnesota

[11] **Dere, A. K.** (2020) Flight Dynamics and Control of The Conventional Aircraft. İstanbul Teknik Üniversitesi, İstanbul.

[12] **Giannelis, N.F.; Bykerk, T.; Vio, G.A. A,** (2023) Generic Model for Benchmark Aerodynamic Analysis of Fifth-Generation High-Performance Aircraft. https://zenodo.org/communities/ssam_gen5/.

[13] **Nguyen, L.T., Ogburn, M.E., Gilbert, W.P., Kibler, K., Brown, P.W., & Deal, P.L.** (1979). Simulator study of stall/post-stall characteristics of a fighter airplane with relaxed longitudinal static stability. [F-16]. Aerospace 2023, 10, 746. https://10.3390/aerospace10090746

[14] **Sonneveldt, L.** (2006). Nonlinear F-16 Model Description.

[15] **De Marco, A., Duke E. and Berndt, Jon.** (2007) "A General Solution to the Aircraft Trim Problem," AIAA 2007-6703. *AIAA Modeling and Simulation Technologies Conference and Exhibit*. August 2007.

[16] **van den Bergen, G.** (2004). *Collision Detection in Interactive 3D Environments*. Morgan Kaufmann.

[17**] Ericson, C.** (2005). *Real-Time Collision Detection*. CRC Press.

[18] **Gottschalk, S., Lin, M. C., & Manocha, D.** (1996). OBBTree: A Hierarchical Structure for Rapid Interference Detection. *Proceedings of the 23rd Annual Conference on Computer Graphics and Interactive Techniques* (SIGGRAPH '96), 171–180. https://doi.org/10.1145/237170.237244

[19] **Eberly, D.** (2001). *3D Game Engine Design: A Practical Approach to Real-Time Computer Graphics*. Morgan Kaufmann.

**CURRICULUM VITAE**

**Name Surname : Ahmet Kutsay DERE**

**EDUCATION:**

- **B.Sc. :** 2020, Istanbul Technical University, Faculty of Aeronautical and Astronautical Engineering, Department of Aeronautical Engineering

**PROFESSIONAL EXPERIENCE AND REWARDS:**

- 2021 – Present: Senior Design Engineer, Turkish Fighter Project, Turkish Aerospace

**PUBLICATIONS, PRESENTATIONS AND PATENTS ON THE THESIS:**

- **Dere A.K,** Acar H**.,** 2025: External Store Separation From Fighter Aircraft. 4rd International Graduate Research Symposium (IGRS'25), May 12-14, 2025, Istanbul, Türkiye.